Article

Cell

Methyltransferase SETD2-Mediated Methylation of STAT1 Is Critical for Interferon Antiviral Activity

Graphical Abstract

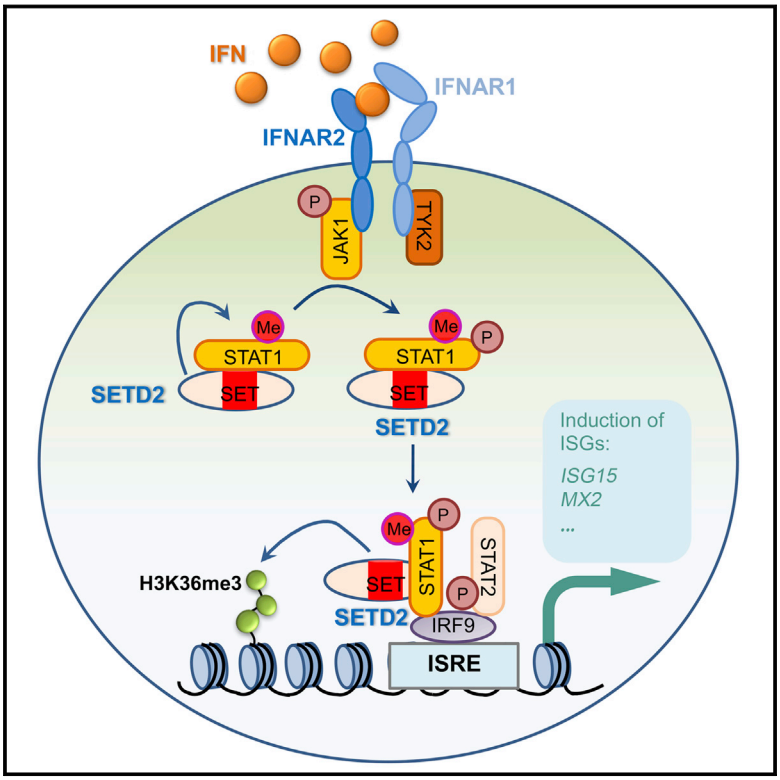

Authors

Kun Chen, Juan Liu, Shuxun Liu, ..., Yingming Jiang, Chunmei Wang, Xuetao Cao

Correspondence

caoxt@immunol.org

In Brief

Multilayer epigenetic modulations of IFNα-dependent signaling responses by the methyltransferase SETD2 are essential for the amplification of antiviral immunity.

Highlights

- SETD2 is a critical amplifier of IFNα antiviral immunity
- Loss of SETD2 in hepatocytes promotes HBV infection and, consequently, liver damage
- STAT1 methylation on K525 is necessary for its phosphorylation and activation
- SETD2 enhances antiviral immunity by directly methylating STAT1 on K525

Chen et al., 2017, Cell *170*, 492–506
July 27, 2017
http://dx.doi.org/10.1016/j.cell.2017.06.042

CellPress

Cell

Article

Methyltransferase SETD2-Mediated Methylation of STAT1 Is Critical for Interferon Antiviral Activity

Kun Chen,[1,2] Juan Liu,[2] Shuxun Liu,[2] Meng Xia,[3] Xiaomin Zhang,[2] Dan Han,[1] Yingming Jiang,[2] Chunmei Wang,[3] and Xuetao Cao[1,2,3,4,*]

[1]Institute of Immunology, Zhejiang University School of Medicine, Hangzhou 310058, China
[2]National Key Laboratory of Medical Immunology & Institute of Immunology, Second Military Medical University, Shanghai 200433, China
[3]Department of Immunology & Center for Immunotherapy, Institute of Basic Medical Sciences, Peking Union Medical College, Chinese Academy of Medical Sciences, Beijing 100005, China
[4]Lead Contact
*Correspondence: caoxt@immunol.org
http://dx.doi.org/10.1016/j.cell.2017.06.042

SUMMARY

Interferon-α (IFNα) signaling is essential for antiviral response via induction of IFN-stimulated genes (ISGs). Through a non-biased high-throughput RNAi screening of 711 known epigenetic modifiers in cellular models of IFNα-mediated inhibition of HBV replication, we identified methyltransferase SETD2 as a critical amplifier of IFNα-mediated antiviral immunity. Conditional knockout mice with hepatocyte-specific deletion of *Setd2* exhibit enhanced HBV infection. Mechanistically, SETD2 directly mediates STAT1 methylation on lysine 525 via its methyltransferase activity, which reinforces IFN-activated STAT1 phosphorylation and antiviral cellular response. In addition, SETD2 selectively catalyzes the tri-methylation of H3K36 on promoters of some ISGs such as *ISG15*, leading to gene activation. Our study identifies STAT1 methylation on K525 catalyzed by the methyltransferase SETD2 as an essential signaling event for IFNα-dependent antiviral immunity and indicates potential of SETD2 in controlling viral infections.

INTRODUCTION

Type I interferons (IFNs) display potent antiviral activities via induction of IFN-stimulated genes (ISGs) through the Janus kinase-signal transducer and activator of transcription (JAK-STAT) signaling pathway (Stark and Darnell, 2012; Sadler and Williams, 2008; Schneider et al., 2014). Dysregulation of IFNα signaling has been closely associated with pathogenesis of various infectious and inflammatory disorders (McNab et al., 2015). While the crucial role of IFNα-induced signaling pathways in host antiviral responses is well established, the mechanisms for the regulation of IFNα-triggered STAT signaling and ISGs expression remain to be fully elucidated.

In addition to phosphorylation and ubiquitination, which have been intensively investigated for their essential role in immunological signaling, other "unconventional" post-translational modification (PTM) such as methylation and acetylation are increasingly shown to be involved in appropriate control of immune and inflammatory responses (Biggar and Li, 2015; Cao, 2016; Chen and Dent, 2014; Liu et al., 2016; Mowen and David, 2014). For example, mono-methylation of nuclear factor κB (NF-κB) subunit RelA by methyltransferase SET domain-containing protein 6 (SETD6) on K310 results in inhibition of NF-κB-driven inflammatory responses (Levy et al., 2011); di-methylation of STAT3 on K49 by methyltransferase enhancer of zeste homolog 2 (EZH2) is required for STAT3 activation and interleukin (IL)-6-induced gene transcription (Dasgupta et al., 2015). STAT1 is the key transcription factor downstream of IFN signaling, which associates with STAT2 and IRF9 to form tri-complex or forms a homodimer to activate expression of a set of genes involved in cell proliferation, apoptosis, and immunological processes (Stark and Darnell, 2012). The activation of STAT1 mainly depends on phosphorylation on tyrosine 701 catalyzed by kinase JAK1, which is crucial for IFNα-induced cellular antiviral signaling, however, the function of unconventional PTMs such as methylation in IFNα-triggered STAT activation as well as the crosstalk between different PTMs and the interaction dynamics in this process remain to be fully understood.

Epigenetic modifying factors and enzymes not only exert their "classical" role in controlling gene transcription by mediating covalent modifications of DNA and histone proteins, but also have the capacity to regulate cellular signaling and responses through modification of non-histone substrates (Mowen and David, 2014). Several histone methyltransferases have been shown to regulate IFNα-mediated immune responses via control of expression of ISGs. For example, lysine methyltransferase, SET (Su [var] 3-9, E[z] and trithorax) domain bifurcated 2 (Setdb2), is induced by type I IFN in murine and human macrophages upon influenza A viral infection and catalyzes trimethylation within ISGs promoter regions to suppress ISGs transcription (Kroetz et al., 2015). However, it is unclear whether epigenetic factors might directly modulate PTMs of IFNα-triggered signaling molecules independent of their ISG regulation activity.

Thus, it is urgent to systemically evaluate the roles of epigenetic molecules in IFNα-mediated antiviral activity.

Chronic hepatitis B caused by persistent hepatitis B virus (HBV) infection affects over 350 million people worldwide (Ott et al., 2012). Currently, IFNα is used for the treatment of chronic hepatitis B in clinics. However, IFNα therapy has been shown to be effective in only a minority of HBV-infected patients (Scaglione and Lok, 2012). The mechanism by which IFNα suppresses HBV infection is largely attributed to IFNα-triggered intrinsic immune signaling that induces the production of antiviral proteins (Lucifora et al., 2014; Yan et al., 2015). Therefore, identifying new regulators of IFNα-mediated protective immunity against HBV infection is crucial for a comprehensive understanding of host anti-HBV immune responses and development of new therapeutic strategies to improve the efficacy of IFNα therapy.

Here, we performed a non-biased high-throughput RNAi screening of 711 known epigenetic modifiers for their potential roles in IFNα-mediated inhibition of HBV replication. We identified SET domain containing protein 2 (SETD2, also known as Huntingtin interacting protein B [HYPB]), as a critical effector molecule that promotes IFNα-mediated cellular response against HBV replication. SETD2 is a histone methyltransferase catalyzing tri-methylation of H3K36 (Edmunds et al., 2008) and has been shown to participate in diverse biological processes including alternative splicing (Luco et al., 2010), transcriptional elongation (Carvalho et al., 2013), DNA repair (Carvalho et al., 2014; Li et al., 2013; Pfister et al., 2014), and embryonic differentiation (Zhang et al., 2014). In addition, mutations in SETD2 are associated with progression of several cancers, such as acute lymphoblastic leukemia and clear cell renal cell carcinoma (ccRCC) (Dalgliesh et al., 2010; Zhang et al., 2012; Zhu et al., 2014). Up to now, the role of SETD2 in immunity and inflammation has not been reported, and the function of non-histone methylation by SETD2 remains unclear. In this study, we report a new role for SETD2 in promoting IFNα-induced antiviral immune response by directly methylating STAT1 on lysine 525 and catalyzing H3K36me3 on the promoters of some ISGs (such as *ISG15*) to activate gene transcription. Thus, SETD2 enhances host antiviral immunity by strengthening IFNα signaling both post-translationally and epigenetically.

RESULTS

RNAi Screening Identifies Epigenetic Candidates Regulating IFNα-Mediated Antiviral Response

To explore the epigenetic modifier landscape of antiviral immunity using IFNα-induced anti-HBV immune response as a model, we conducted a high-throughput small hairpin RNA (shRNA) screening in HBV-transfected HepG2.2.15 cells (Sells et al., 1987) using HBsAg secretion in the supernatant after IFNα treatment as the readout. The screening library consists of 1,422 unique shRNA-expressing lentivirus, leading to knockdown of 711 candidate epigenetic regulatory genes (Figure 1A; Table S1). On the basis of fold changes in HBsAg secretion after shRNA transfection, 37 genes were selected as primary hits: silencing of 18 candidate genes, including *PRMD7*, *NAT9*, and *AIP*, enhanced HBsAg secretion by more than 2-fold, whereas silencing of the other 19 genes, including *TGM3* and *PHF8*, inhibited HBsAg secretion (Figure 1B). Among these primary hits, AIP has been previously reported to interact with HBX, directly inhibiting HBsAg secretion (Kuzhandaivelu et al., 1996), thereby confirming the validity of our screening system.

A secondary screen was performed to further validate the 37 primary hits. Three individual small interfering RNAs (siRNAs) were designed for each gene, and candidates were regarded as positive hits if transfection of at least two siRNAs caused significant changes in HBsAg secretion. A total of 21 positive hits were obtained from this secondary screen, including *SETD2*, *ZCCHC4*, *TRIM28*, and *PHF8* (Figure 1C; Tables S2 and S3). Of these 21 genes, our preliminary functional screening showed that HBsAg secretion and intracellular HBV DNA (both indicative of HBV replication) were significantly higher in SETD2-silenced HepG2.2.15 cells as compared to that in control cells in response to IFNα treatment (Figure 1D). HBV replication was also increased in SETD2-silenced HepG2 cells transiently transfected by pHBV1.3 plasmids (Figure 1E). The increase of HBV replication by SETD2 silencing was not due to changes in cell proliferation or IFNα-induced apoptosis (Figures S1A–S1C). Furthermore, by comparing the mRNA level of *SETD2* in liver tissues from 20 HBV-positive (HBV^+) and 10 HBV-negative (HBV^-) patients with hepatocellular carcinoma (HCC) to normal liver tissues from six liver hemangioma patients (with no history of HBV infection), we found that the expression of *SETD2* was significantly lower in HBV^+ samples than that in HBV^- and healthy samples (Figure 1F). Taken together, these data suggest that SETD2 plays a potent role in IFNα-mediated inhibition of HBV replication.

SETD2 in Hepatocytes Promotes IFNα-Mediated Inhibition of HBV Replication via Its SET Domain

We next focused on investigating the structure-function relationship of SETD2 in IFNα-induced antiviral immune response. SETD2 contains a SET domain with the adjacent associate with SET (AWS) and post-SET domain and a WW domain located in the C terminus (Sun et al., 2005). The SET domain has been shown to be the catalytic methyltransferase domain and is considered as the signature motif of methyltransferase (Sun et al., 2005). We constructed vectors encoding 1–945 amino acids (aa), 946–1738 aa (containing the SET domain), and 1739–2565 aa of SETD2 and named them fragment 1, 2, and 3, respectively (Figure 2A). Overexpression of the SETD2-fragment 2 (F2), but not SETD2-F1 or SETD2-F3, significantly promoted IFNα-mediated suppression of HBV replication (Figure 2A), suggesting that SETD2 enhances anti-HBV activity of IFNα via its SET domain.

To determine the in vivo effect of SETD2 on IFNα antiviral activity, we co-injected HBV-expressing plasmid (pHBV1.3) and SETD2-F2-expressing plasmid into C57BL/6 mice by hydrodynamic tail vein (HTV) injection that has been reported to be a mouse model of acute HBV infection (Yang et al., 2002). Consistent with the in vitro results, overexpression of the SET domain-containing SETD2-F2 potently reduced serum HBsAg titers (Figure 2B) and significantly decreased the densities of hepatitis B core antigen (HBcAg)-expressing hepatocytes in HBV-injected wild-type mice (Figure 2C). However, overexpression of SETD2-F2 did not inhibit HBV replication in mice deficient in IFNα

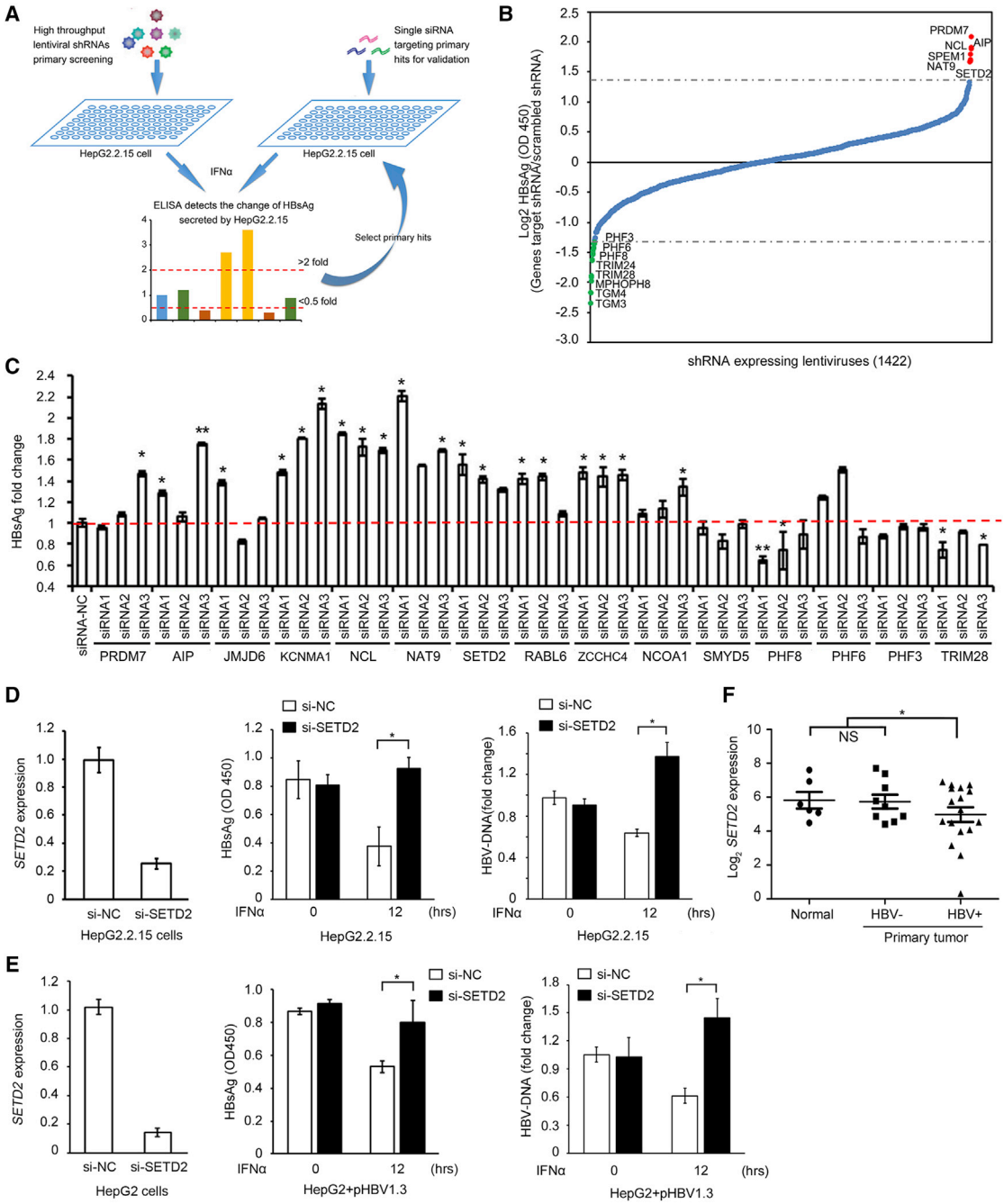

Figure 1. RNAi Screening Identifies Epigenetic Candidates Involved in Regulation of IFNα-Mediated Inhibition of HBV Replication

(A) Diagram of the two-stage screening strategy by lentivirus-mediated shRNA library and siRNA validation.

(B) Fold changes of HBsAg secretion of HepG2.2.15 cells transfected with 1,422 targeting shRNAs followed by 1,000 U/mL IFNα treatment for 12 hr. Targeted genes that significantly increased or decreased HBsAg secretion are highlighted in red or green, respectively.

(C) Fold changes of HBsAg secretion of HepG2.2.15 cells transfected with siRNAs for secondary validation followed by IFNα treatment as in (B). Data are normalized to unstimulated HepG2.2.15 cells (dotted line).

(D) qRT-PCR analysis of *SETD2* expression (left), HBV relaxed circular DNA (rcDNA) (right), and ELISA of HBsAg secretion (middle) of HepG2.2.15 cells transfected with scrambled siRNA (si-NC) or siRNA specific for *SETD2* (si-SETD2), followed by IFNα treatments as in (B).

(E) qRT-PCR analysis of *SETD2* expression (left), HBV-DNA (right), and ELISA of HBsAg secretion (middle) of HepG2 cells co-transfected with pHBV1.3 plasmids and si-NC or si-SETD2, followed by IFNα treatment as in (B).

(F) qRT-PCR analysis of *SETD2* expression in HBV-positive HCC tissues (n = 20), HBV negative HCC issues (n = 10), and normal liver tissues (n = 6).

Data are shown as mean ± SD of three independent experiments. *p < 0.05, **p < 0.01. NS, not significant. See also Tables S1, S2, and S3.

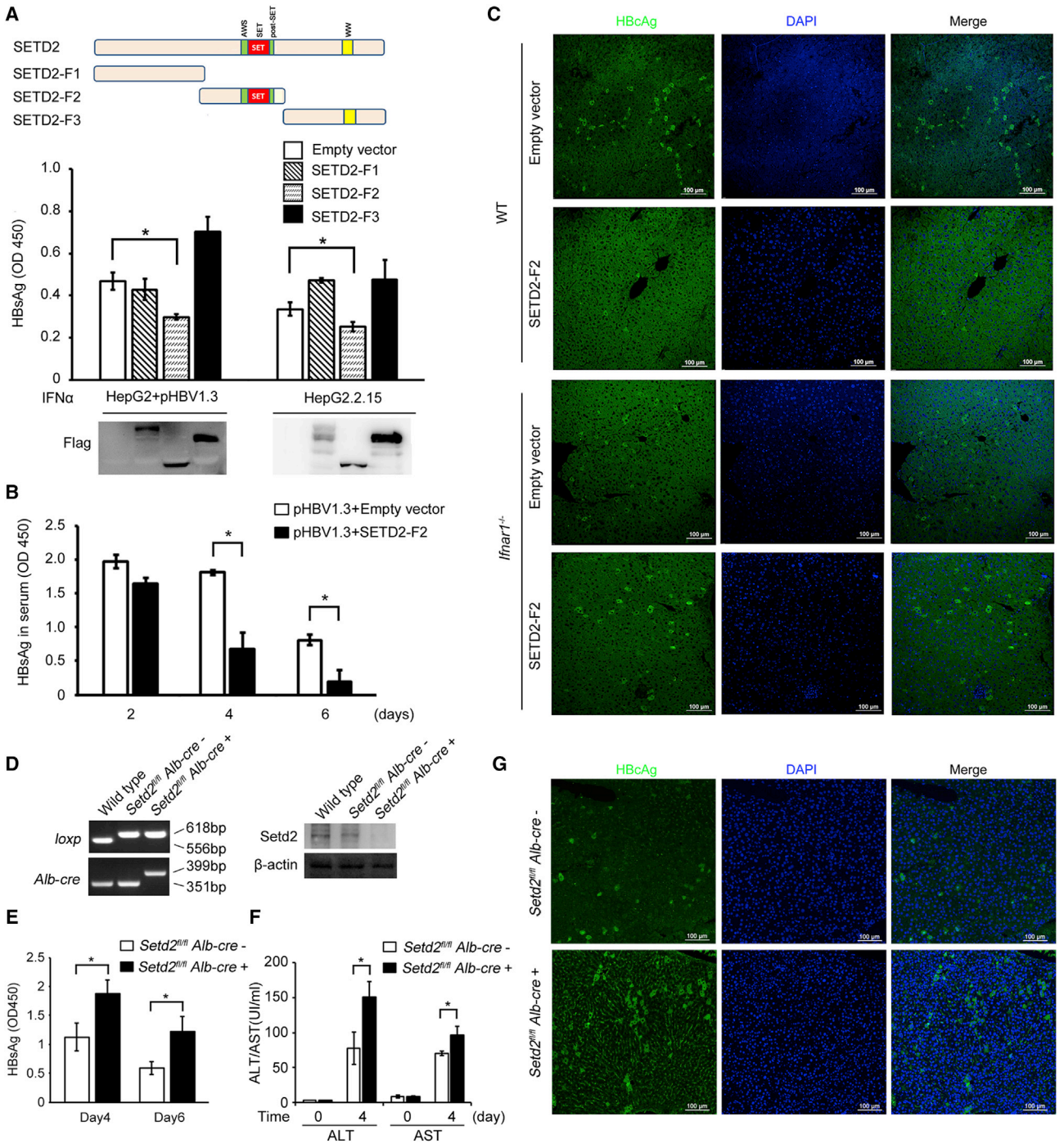

Figure 2. SETD2 in Hepatocytes Promotes IFNα-Mediated Inhibition of HBV Replication

(A) Schematic diagram showing SETD2 major domains and the truncated fragments (top). ELISA of HBsAg titer in supernatants of pHBV1.3 transfected HepG2 cells and HepG2.2.15 cells after transfection with flag-tagged SETD2 truncation expressing plasmids and treatment with IFNα for 12 hr (middle). Immunoblot analysis of flag-proteins in whole-cell lysates of HepG2 and HepG2.2.15 cells transfected as in the middle panel (bottom).

(B) ELISA of serum HBsAg in mice at indicated time after HTV-injection with pHBV1.3 and empty vector or flag-tagged SETD2-F2 expression plasmids. Data are shown as mean ± SD (n = 6). *$p < 0.05$.

(C) Immunofluorescence in pronase-digested paraffin sections of liver biopsies from HTV-injected mice as in (B), stained with HBcAg primary antibody, and detected with fluorescein isothiocyanate (FITC)-labeled anti-mouse IgG. Scale bars, 100 μm.

(D) PCR analysis of *loxp* and *cre* genes in genomic DNA (left) and immunoblot analysis of Setd2 in lysates of primary hepatocytes (right) from wild-type C57BL/6 mice, *Setd2*$^{fl/fl}$ Alb-cre^{-}, and *Setd2*$^{fl/fl}$ Alb-cre^{+} mice. β-actin was used as loading control.

(legend continued on next page)

receptor (*Ifnar1*$^{-/-}$) (Figure 2C). Furthermore, overexpression of SETD2-F2 significantly reduced the serum aspartate transaminase (AST) and alanine aminotransferase (ALT) levels in HBV-injected wild-type mice, but not in HBV-injected *Ifnar1*$^{-/-}$ mice (Figure S1D). Therefore, SETD2 promotes IFNα-mediated inhibition of HBV replication both in vitro and in vivo via its SET domain.

SET domain proteins can be classified into seven subfamilies with different substrate selectivity depending on the sequences around SET domain. SETD2 and four other SET domain proteins including nuclear receptor binding SET domain protein (NSD1), NSD2, NSD3, and absent, small, or homeotic-like (*Drosophila*) (ASH1L), belong to the SET2 subfamily (Cheng et al., 2005). Among all the SET2 subfamily members, SETD2 shares the highest homology with ASH1L. Therefore, we wondered whether SET domains of ASH1L may have similar effect in promoting IFNα activity as the SET domain of SETD2. Unlike SET domain-containing fragments of SETD2, overexpression of SET domain-containing fragments of Ash1l (1886–2958 aa) had no effect in IFNα-mediated inhibition of HBV either in vitro (Figure S1E) or in vivo (Figure S1F). These results indicate a unique role of SET domain-containing SETD2-F2 in promoting IFNα antiviral activity that is not shared by other SET domain-containing proteins. This is likely due to the special spatial configuration of SET domains in SETD2 consisting of three discrete β sheets arranged in a triangular shape, which significantly differs from other SET domains of other proteins (Yang et al., 2016).

We then generated *Setd2* conditional knockout mice with hepatocyte-specific deletion of *Setd2* (*Setd2*$^{fl/fl}$ Alb-cre^{+}) through homologous recombination and confirmed the deficiency of *Setd2* expression in hepatocytes of *Setd2*$^{fl/fl}$ Alb-cre^{+} as compared to that of *Setd2*$^{fl/fl}$ Alb-cre^{-} control mice (Figure 2D). Notably, after HBV infection, *Setd2*$^{fl/fl}$ Alb-cre^{+} mice showed elevated HBsAg titers (Figure 2E), higher ALT and AST levels in serum (Figure 2F), as well as increased HBcAg expression in hepatocytes (Figure 2G) as compared to *Setd2*$^{fl/fl}$ Alb-cre^{-} mice. These in vivo data indicate that hepatocyte-specific deficiency of *Setd2* leads to enhanced HBV infection and more severe liver injury in vivo and further demonstrated that SETD2 in hepatocytes promotes innate defense against HBV infection in vivo.

SETD2 Enhances IFNα-Induced Antiviral Function by Promoting STAT1 Activation via SET Domain-Containing Fragment

IFNα induces STAT1 phosphorylation and subsequently initiates transcription of a set of IFN-stimulated genes (ISGs) contributing to antiviral immunity. We therefore tested whether SETD2 regulates IFNα-triggered signaling. Indeed, in response to IFNα stimulation, the levels of STAT1 (but not STAT2) phosphorylation and H3K36me3 (Figure 3A), STAT1 nuclear translocation (Figure 3B), and *ISG15* mRNA expression (Figure 3C) were significantly reduced in SETD2-silenced HepG2 cells as compared to that in control HepG2 cells. Furthermore, in response to murine IFNα stimulation, the STAT1 phosphorylation and H3K36me3 levels (Figure 3D) and *Isg15* mRNA expression (Figure 3E) were significantly reduced in primary hepatocytes from *Setd2*$^{fl/fl}$ Alb-cre^{+} mice than that in primary hepatocytes from *Setd2*$^{fl/fl}$ Alb-cre^{-} mice. Therefore, SETD2 significantly promotes IFNα-triggered STAT1 signaling and ISG expression in both HepG2 cells and primary hepatocytes.

We then utilized CRISPR/Cas9 technology to knock out SETD2 in HepG2 cells, generating three SETD2-KO cell lines via targeting three distinct exons: exon1, exon3, and exon9 (Figure S2A). Each clonal cell line harbors a frameshift mutation in both SETD2 alleles (Figures S2B–S2D), resulting in loss of *SETD2* expression (Figure S2E) and decreased total H3K36me3 levels (Figure 3F). All three SETD2-KO HepG2 cell lines showed impaired phosphorylation of STAT1 induced by IFNα as compared to control HepG2 cells (Figures 3G and S2F). No significant difference in the expression of *IFNAR1/R2* or STAT1 upstream signaling molecules such as tyrosine kinases Janus kinase 1 (*JAK1*) and tyrosine kinase 2 (*TYK2*) were observed in IFNα-treated SETD2-KO HepG2 cells (data not shown). Through RNA sequencing (RNA-seq) analysis, we found that the expression of a set of ISGs was lower in SETD2-KO cells than that in HepG2 WT cells in response to IFNα stimulation (Figure 3H). qRT-PCR analysis confirmed reduced expression of two ISGs, including *ISG15* and *MX2* after IFNα stimulation in SETD2-KO cells (Figure 3I). In response to stimuli with other subtypes of IFNs including IFNβ, IFNγ, and IFNλ, the levels of STAT1 phosphorylation, H3K36me3 (Figure S3A), and *ISG15* mRNA expression (Figure S3B) were also reduced in SETD2-KO cells than that in HepG2 WT cells. Therefore, SETD2 enhances STAT1 phosphorylation and ISG expression triggered by all types of IFNs.

We next performed rescue experiments using SETD2 or STAT1 overexpression plasmids to further elucidate SETD2-mediated regulation of IFN signaling. Overexpression of the SET domain-containing SETD2-F2, but not other fragments (SETD2-F1 and SETD2-F3), in SETD2-KO cells upregulated IFNα-induced *ISG15* expression (Figure 3J) and H3K36 methyltransferase activity (Figure 3K). We also generated STAT1-knockout (STAT1-KO) cell lines using CRISPR/Cas9 targeting exon6 of STAT1 and confirmed the loss of STAT1 protein in STAT1-KO cells (Figure S3C). We then generated an active mutation of STAT1 with substitution of cysteine for alanine at positions 656 and 658 (STAT1-CC) that constantly enhanced

(E) ELISA of serum HBsAg in *Setd2*$^{fl/fl}$ Alb-cre^{-} and *Setd2*$^{fl/fl}$ Alb-cre^{+} mice after HTV-injection with pHBV1.3 plasmid for indicated time. Data are shown as mean ± SD (n = 6). *p < 0.05.

(F) ELISA of AST and ALT in sera from *Setd2*$^{fl/fl}$ Alb-cre^{-} and *Setd2*$^{fl/fl}$ Alb-cre^{+} mice after HTV injection with pHBV1.3 plasmids for indicated time. Data are shown as mean ± SD (n = 6). *p < 0.05.

(G) Immunofluorescence in pronase-digested paraffin sections of liver biopsies from HTV-injected *Setd2*$^{fl/fl}$ Alb-cre^{-} and *Setd2*$^{fl/fl}$ Alb-cre^{+} mice, stained and detected as in (C). Scale bars, 100 μm.

Data are shown as mean ± SD of three independent experiments (A) or shown for one representative experiment from three independent experiments with similar results. *p < 0.05, **p < 0.01. See also Figures S1 and S2.

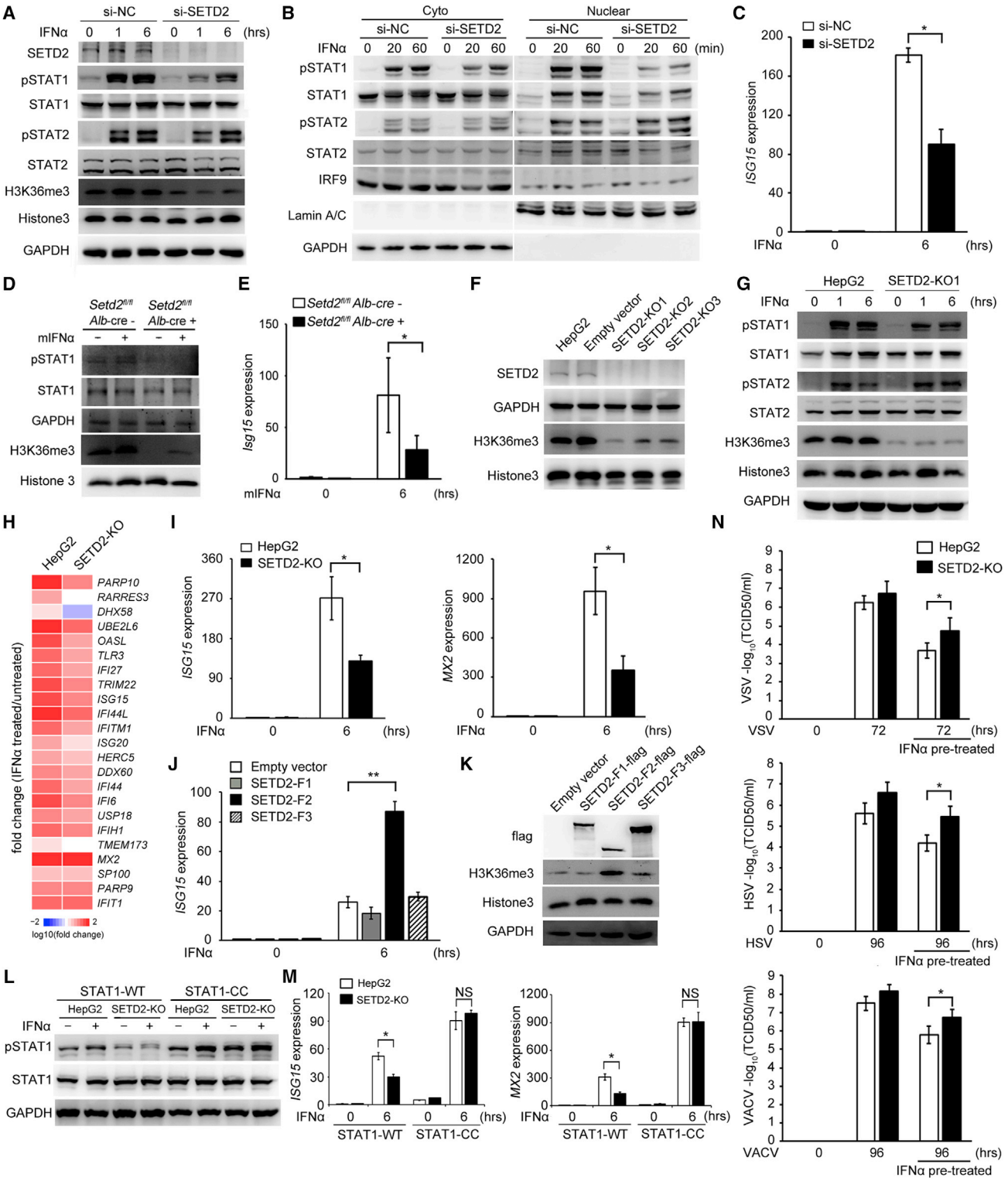

Figure 3. SETD2 Facilitates IFNα-Induced STAT1 Phosphorylation and ISGs Expression

(A) IB analysis of phosphorylated (p)STAT1, pSTAT2, SETD2, STAT1, STAT2, H3K36me3, and Histone3 in lysates of HepG2 cells transfected with si-NC or si-SETD2 followed by 1,000 U/mL IFNα treatment for the indicated time. GAPDH was used as a control.

(B) IB analysis of pSTAT1, pSTAT2, STAT1, and STAT2 in cytoplasmic and nuclear extracts of HepG2 cells transfected and stimulated as in (A). GAPDH and Lamin A/C were used as the cytoplasmic and nuclear controls, respectively.

(legend continued on next page)

IFN-induced expression of *ISG15* and *MX2* and STAT1 phosphorylation in STAT1-KO cells (Zhang et al., 2015b) (Figures S3D and S3E). Overexpression of STAT1-CC could significantly enhance IFNα-induced STAT1 phosphorylation (Figure 3L) and upregulate IFNα-induced *ISG15* and *MX2* mRNA expression (Figure 3M) in both HepG2 cells and SETD2-KO cells. These results further indicated that SETD2 enhances IFNα-induced ISG expression by promoting STAT1 activation via SET domain-containing fragment.

We then analyzed whether SETD2 could regulate innate defense against different types of virus infection. Upon infection with DNA virus herpes simplex virus (HSV), vaccinia virus (VACV), and also RNA virus VSV, the viral titers and replications in SETD2-KO HepG2 cells, in the absence of IFNα pretreatment, remained almost unchanged compared to that in control HepG2 cells. By contrast, viral titers and replications in SETD2-KO HepG2 cells, in the presence of IFNα pretreatment, were increased at least ten times more than in control cells (Figures 3N and S3F), indicating the important role of SETD2 in IFNα-mediated antiviral effect. Collectively, SETD2 is critical for optimal activation of IFNα-dependent STAT1 activation and ISG expression and for efficient innate defense against different types of virus.

SETD2 Directly Induces Mono-methylation of STAT1 via Methyltransferase Activity

The above data suggest that SETD2 enhances STAT1 phosphorylation and nuclear translocation in response to IFNα. Because several histone methyltransferases have been shown to mediate methylation of non-histones and thus affect protein function and signaling transduction (Dasgupta et al., 2015; Levy et al., 2011), we asked whether SETD2 mediates methylation of signaling molecules such as STAT1 to affect its activity. Interestingly, IFNα stimulation induced mono-methylation of STAT1 (Figure 4A). Silencing of SETD2 reduced IFNα-induced STAT1 mono-methylation in HepG2 cells (Figure 4B), whereas overexpression of the SET domain containing SETD2-F2 led to increased mono-methylation and phosphorylation of STAT1 than SETD2-F3 (Figure 4C).

It has been reported that mutation of arginine (R) 196 and cysteine (C) 202 in the SET domain of yeast SET2 abrogates methyltransferase function (Rea et al., 2000). Using sequence homology comparison, we found that these two residues are evolutionarily conserved, and R1625 and C1631 in human are homologous to R196 and C202 in yeast (Figure 4D). We transfected the SET domain-containing SETD2-F2 with R1625G or C1631A point mutations into SETD2-KO HepG2 cells and found that the R1625G SETD2 fragment abolished H3K36me3 methyltransferase activity, whereas C1631A did not affect H3K36me3 levels (Figures 4D and 4E). While SETD2-F2 enhanced mono-methylation and phosphorylation of STAT1, the methyltransferase-dead SETD2-F2 (R1625G) lost the ability to enhance STAT1 mono-methylation and phosphorylation (Figure 4F). In addition, co-immunoprecipitation experiments in HEK293T cells suggested that SETD2-F2, but not other fragments, interacted with STAT1 (Figure 4G). Although the expression of SETD2 itself was not upregulated by IFNα, the interaction between SETD2-F2 and STAT1 was dependent on IFNα stimulation (Figure 4H). These data suggest SETD2 interacts with STAT1 upon IFNα stimulation to induce mono-methylation of STAT1 via methyltransferase activity.

We also constructed a group of glutathione S-transferase (GST)-fusion proteins respecting different SETD2 truncations (SETD2 T1–T6) and 6× his-fusion full-length STAT1 and detected a direct and specific interaction between SETD2-T3 and STAT1 proteins (Figure 4I). We then further divided SETD2 T3 and T4 into N-terminal and C-terminal (T3N, T3C, T4N, and T4C), respectively, to determine the exact region in SETD2 that interacts with STAT1 (Figure 4J). Pull-down assay demonstrated that SETD2 T3C and T4N, both containing SET domain, bind to STAT1 (Figure 4J), indicating SET domain was sufficient for interaction with STAT1. However, we did not observe the interaction between STAT1 and SETD2 T4 that also contains SET domain. This might be due to the low expression efficiency of SETD2 T4 protein (Figure 4I). Taken together, these results suggest that SETD2 interacts with STAT1 to mediate its methylation via the methyltransferase activity in response to IFNα stimulation.

(C) qRT-PCR analysis of *ISG15* expression in HepG2 cells transfected and stimulated as in (A).
(D) IB analysis of pSTAT1, STAT1, H3K36me3, and Histone3 in hepatocytes from *Setd2*$^{fl/fl}$ Alb-cre^{-} and *Setd2*$^{fl/fl}$ Alb-cre^{+} mice stimulated with 200 U/mL recombinant murine IFNα (mIFNα) in vitro for 1 hr.
(E) qRT-PCR analysis of *Isg15* expression in hepatocytes from *Setd2*$^{fl/fl}$ Alb-cre^{-} and *Setd2*$^{fl/fl}$ Alb-cre^{+} mice stimulated with 200 U/mL mIFNα in vitro for 6 hr.
(F) IB analysis of SETD2, H3K36me3, and Histone3 in whole-cell lysates of control and SETD2-KO HepG2 cells lines generated by three different CRISPR target sites named SETD2-KO1, SETD2-KO2, and SETD2-KO3.
(G) IB analysis of pSTAT1, pSTAT2, STAT1, STAT2, H3K36me3, and Histone3 in whole-cell lysates of control and SETD2-KO HepG2 cells stimulated as in (A).
(H) Heatmap of the upregulated genes in HepG2 cells or SETD2-KO cells stimulated with IFNα for 6 hr relative to those in the cells without IFNα treatment. Log10 (fold change) values were calculated from fragments per kilobase of transcript per million (FPKM) values of RNA-seq.
(I) qRT-PCR analysis of *ISG15* and *MX2* expression in control and SETD2-KO HepG2 cells upon IFNα treatment.
(J) qRT-PCR analysis of *ISG15* expression in SETD2-KO HepG2 cells rescued with different SETD2 truncated expression plasmids upon IFNα treatment.
(K) IB analysis of H3K36me3 levels in SETD2-KO HepG2 cells transfected as in (J).
(L) IB analysis of pSTAT1, STAT1 in lysates of control, and SETD2-KO HepG2 cells rescued with STAT1-WT or STAT1-CC expression plasmids upon IFNα treatment.
(M) qRT-PCR analysis of *ISG15* and *MX2* expression in WT and SETD2-KO HepG2 cells rescued and stimulated as in (L).
(N) $TCID_{50}$ assay of VSV, HSV, and VACV titer in supernatants of control and SETD2-KO HepG2 cells pre-treated with or without IFNα for indicated time followed by VSV, HSV, and VACV infection for 24 hr.
Data are shown as mean ± SD of three independent experiments (C, E, I–K, M, N) or shown for one representative experiment from three independent experiments with similar results. *$p < 0.05$, **$p < 0.01$. NS, not significant. See also Figure S3.

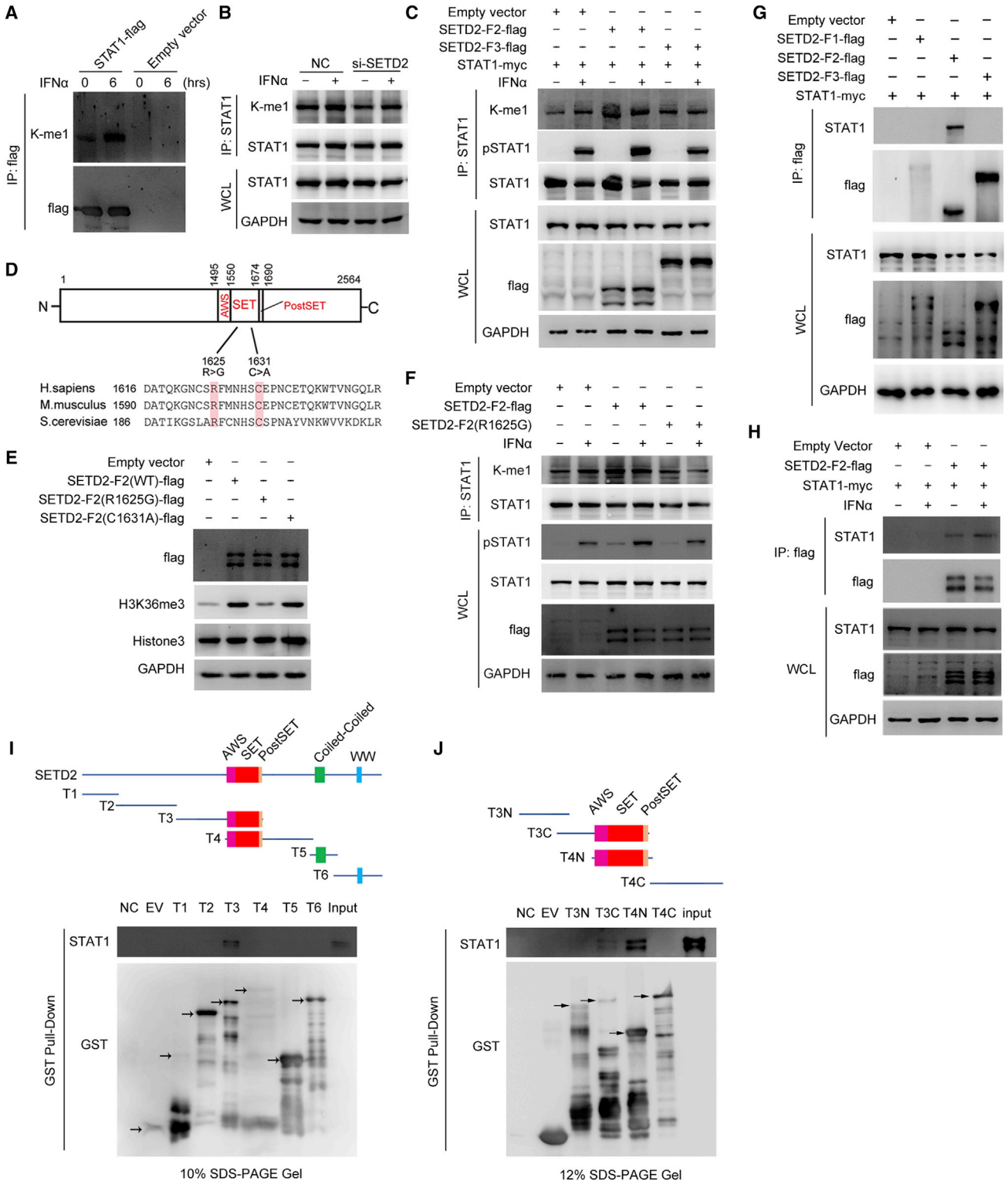

Figure 4. SETD2 Induces Mono-methylation of STAT1 via Its SET Domain Methyltransferase Activity

(A) IB analysis of mono-methylation of STAT1 in immunoprecipitates of HEK293T cells transfected with flag-tagged STAT1 expression plasmids or empty vector and then treated with 1,000 U/mL IFNα for the indicated time.

(B) IB analysis of mono-methylation of STAT1, STAT1 in immunoprecipitates, and whole-cell lysates of HepG2 cells transfected with si-NC or si-SETD2 followed by IFNα treatment as in (A).

(legend continued on next page)

Methylation of Lysine 525 of STAT1 Is Necessary for Its Phosphorylation and Transcriptional Activity

The above data suggest that SETD2 directly interacts with STAT1 and mediates its methylation in response to IFNα stimulation. To confirm the direct interaction between SETD2 and STAT1 and subsequent methylation of STAT1, we performed mass spectrometry (MS) analysis and systemically identified potentially methylated lysine residues of STAT1 induced by IFNα (Figure S4A). A total of seven mono-methylated lysine residues (K114, K175, K296, K366, K525, K637, and K665) were identified (Figures 5A, 5B, and S4B). However, di- and tri-methylation on lysine residues of STAT1 were not detected in our MS analysis.

To further investigate the effect of methylation on STAT1 activity, we constructed STAT1 mutations with all the MS-identified methylated lysine residues (K) replaced with alanine (A), as well as a double-site mutation on K636/K637. Out of the eight lysine to alanine mutants tested, only the overexpression of STAT1 K525A led to significantly reduced IFNα-induced STAT1 phosphorylation on tyrosine 701 (Figure 5C) and nuclear translocation (Figure 5D) as well as decreased expression of ISGs including *ISG15*, *IFIT-1*, and *MX2* (Figure 5E) in STAT1-KO cells. The interaction between JAK1 and STAT1 by IFNα stimulation was reduced by STAT1-K525A mutation in both HepG2 cells and human primary macrophages derived from $CD14^+$ human peripheral blood monocytes cultured in M-CSF (Figures 5F and S5A). Moreover, electrophoretic mobility shift assay (EMSA) with biotin-labeled single ISRE or GAS probes showed that K525A-mutated STAT1 showed significantly less binding with ISRE and GAS elements (Figure 5G). Unexpectedly, K525A mutation did not influence homo-dimerization of STAT1 (Figure S5B), hetero-dimerization of STAT1 and STAT2 (Figure S5C), nor the interaction between STAT1 and IRF9 (Figure S5D). It was shown that both phosphorylated and unphosphorylated STAT1 can dimerize or interact with STAT2 and IRF9 (Cheon and Stark, 2009; Sung et al., 2015), which may partially explain why K525 mutation inhibited STAT1 phosphorylation, but did not affect STAT1 dimerization and STAT2 or IRF9 interaction. It will be intriguing to further clarify the detailed mechanisms involved in the differential effect of STAT1 K525me1 in its molecular interactions. Collectively, these data demonstrate that K525 of STAT1, which is a critical methylation lysine residue on STAT1, is required for IFNα-induced STAT1 interaction with JAK1 and for the phosphorylation, nuclear translocation, and DNA binding activity of STAT1 as well as for the subsequent expression of ISGs.

SETD2 Directly Mediates Mono-Methylation of STAT1 on K525

We next sought to determine whether SETD2 is necessary and sufficient for STAT1 K525me1. While mutation of K525 decreased the level of mono-methylation of STAT1 upon IFNα stimulation (Figure 6A), SETD2-F2 overexpression significantly enhanced STAT1 mono-methylation in STAT1-KO cells rescued with overexpression of STAT1 but not in STAT1-KO cells rescued with overexpression of STAT1 K525A mutation (Figure 6B).

To further validate these data in vivo, we induced lentivirus-mediated stable expression of STAT1-WT (WT-Re) or STAT1-K525A (K525A-Re) in STAT1-KO cells. In line with the reduced STAT1 activation, ISG expression and viral resistance in SETD2-KO cells (Figures 3G, 3I, and 3N), STAT1-K525A-Re cells also had reduced STAT1 phosphorylation (Figure S6A), ISGs expression (Figure S6B), and impaired resistance to viral infection (Figure S6C) as compared to that in WT-Re cells in response to IFNα stimulation. Furthermore, we generated a specific polyclonal antibody against a STAT1 K525me1 peptide. Dot blot analysis demonstrated minimal cross-reactivity of the polyclonal antibody with un-methylated K525 containing peptide (Figure S6D). Western blot with the specific K525me1 antibody showed that methylation of this lysine residue of STAT1 could be induced by IFNα or IFNγ, which was significantly decreased in K525A-Re cells as compared to that in WT-Re cells (Figure 6C and S6E). Importantly, silencing of SETD2 significantly reduced K525me1 of STAT1 in HepG2 cells induced by IFNα (Figure 6D). Because SETD2 not only catalyzes trimethylation of H3K36 but also mono- and di-methylation of H3K36 (Yuan et al., 2009), we next investigated whether SETD2 could directly methylate STAT1. In the in vitro methylation assay, we used purified STAT1 or histone as the substrate, S-adenosyl-L-methionine (SAM) as the methyl group donor, and purified GST-tagged SETD2 T4N (mainly SET domain) as the enzyme. We found that SETD2 could indeed directly catalyze both K525me1 of STAT1 and H3K36me3 of histones (Figures 6E and S6F). In line with the importance of K525 of STAT1 for its interaction with JAK1, SETD2-KO cells also showed reduced interactions between endogenous STAT1 and JAK1, but intact STAT1-STAT2 or STAT-IRF9 interactions in response to IFNα or IFNβ stimulation (Figures 6F and 6G). Taken together, these results indicate that methyltransferase SETD2 directly mediates mono-methylation of K525 of STAT1, which is an important PTM enhancing STAT1 activation and expression of ISGs.

(C) IB analysis of mono-methylation of STAT1 and total STAT1 in immunoprecipitates of HEK293T cells co-transfected with myc-tagged STAT1 expression plasmids and flag-tagged SETD2 truncation expression plasmids followed by IFNα treatment as in (A).
(D) Schematic diagram showing mutation sites in SETD2.
(E) IB analysis of H3K36me3 in whole-cell lysates of SETD2-KO cells transfected with flag-tagged SETD2-F2 or mutated SETD2-F2 expression plasmids.
(F) IB analysis of mono-methylation of STAT1 in immunoprecipitates of HepG2 cells transfected with flag-tagged SETD2-F2 and mutated SETD2-F2 expression plasmids followed by IFNα treatment as in (A).
(G) IB analysis of STAT1 in immunoprecipitates of HEK293T cells co-transfected with myc-tagged STAT1 and flag-tagged SETD2 truncation expression plasmids.
(H) IB analysis of STAT1 in immunoprecipitates of HEK293T cells co-transfected with myc-tagged STAT1 and flag-tagged SETD2-F2 expression plasmids stimulated with IFNα.
(I) IB analysis of STAT1 and Coomassie blue staining analysis of GST-SETD2 truncation (T1–T6) expression in a GST pull-down assay.
(J) IB analysis of STAT1 and Coomassie blue staining analysis of GST-SETD2 truncation (T3N, T3C, T4N, T4C) expression in a GST pull-down assay.
Data are shown for one representative experiment. Similar results were obtained in three independent experiments.

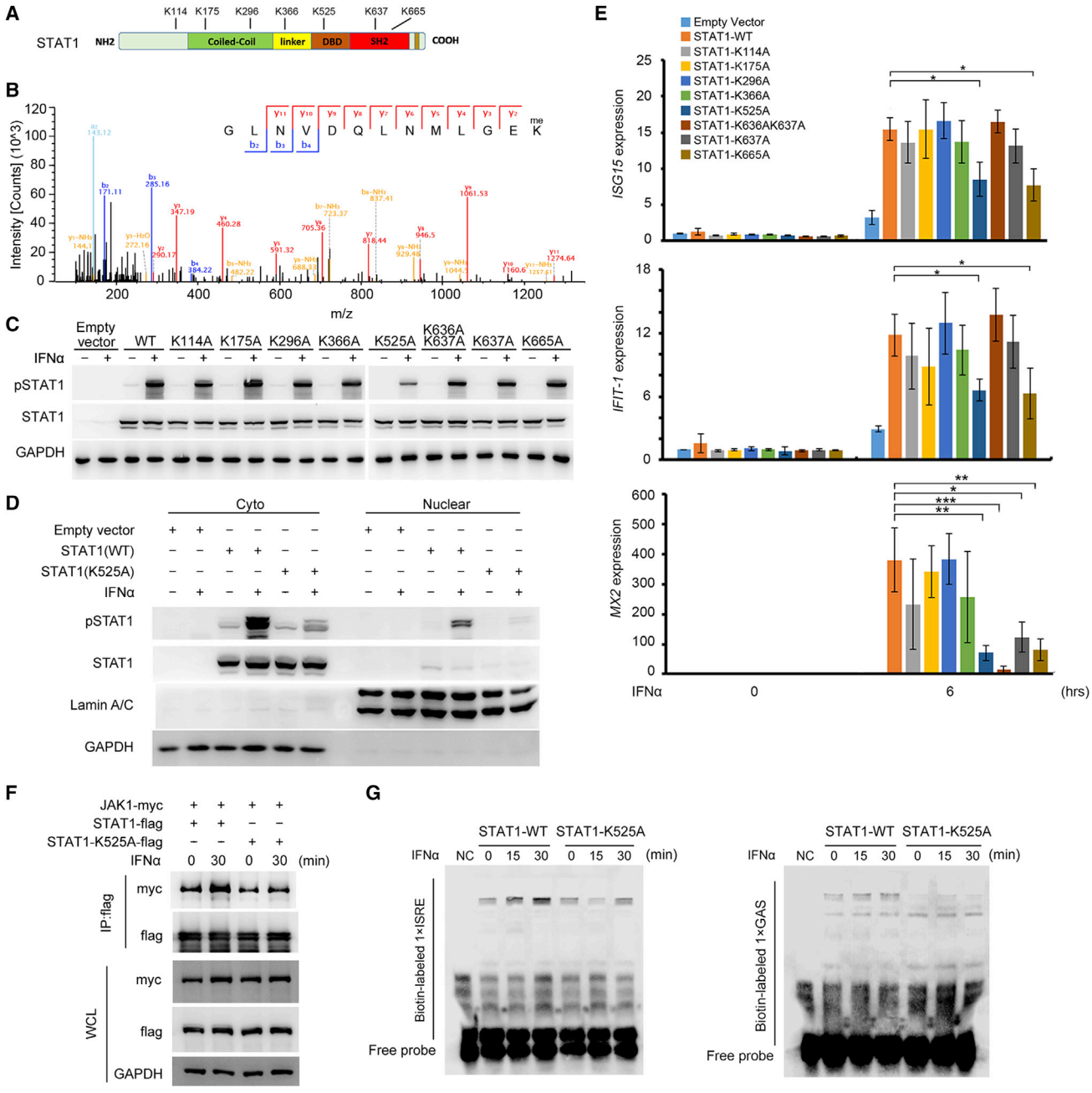

Figure 5. Methylated Lysine 525 of STAT1 Is Necessary for Its Phosphorylation and Transcriptional Activity

(A) Identification of methylated lysine residues in STAT1 in HepG2 cells by immunoprecipitation combined with mass spectrometry.

(B) Tandem mass spectrometry of STAT1 peptide modified with methylation on lysine 525 residue.

(C) IB analysis of pSTAT1 and total STAT1 in whole-cell lysates of STAT1-KO HepG2 cells transfected with wild-type STAT1 (STAT1-WT) or point mutated STAT1 expression plasmids, followed by 1,000 U/mL IFNα treatment for 6 hr.

(D) IB analysis of pSTAT1 and total STAT1 in nuclear and cytoplasmic (cyto) extracts of STAT1-KO cells transfected with STAT1-WT or STAT1-K525A expression plasmids and stimulated as in (C).

(E) qRT-PCR analysis of *ISG15*, *IFIT-1*, and *MX2* expression in STAT1-KO cells treated as in (C).

(F) IB analysis of immunoprecipitates of STAT1-KO HepG2 cells co-transfected with myc-tagged JAK1 and flag-tagged STAT1-WT or STAT1-K525A expression plasmids followed by IFNα treatment for 30 min.

(G) EMSA of whole-cell lysates from STAT1-KO cells transfected as in (C) and treated with IFNα for indicated time. 1× ISRE motif and 1× GAS motif were biotin-labeled.

Data are representative photographs of three independent experiments with similar results or shown as mean ± SD of three independent experiments (E). *p < 0.05, **p < 0.01, ***p < 0.001. See also Figures S4 and S5.

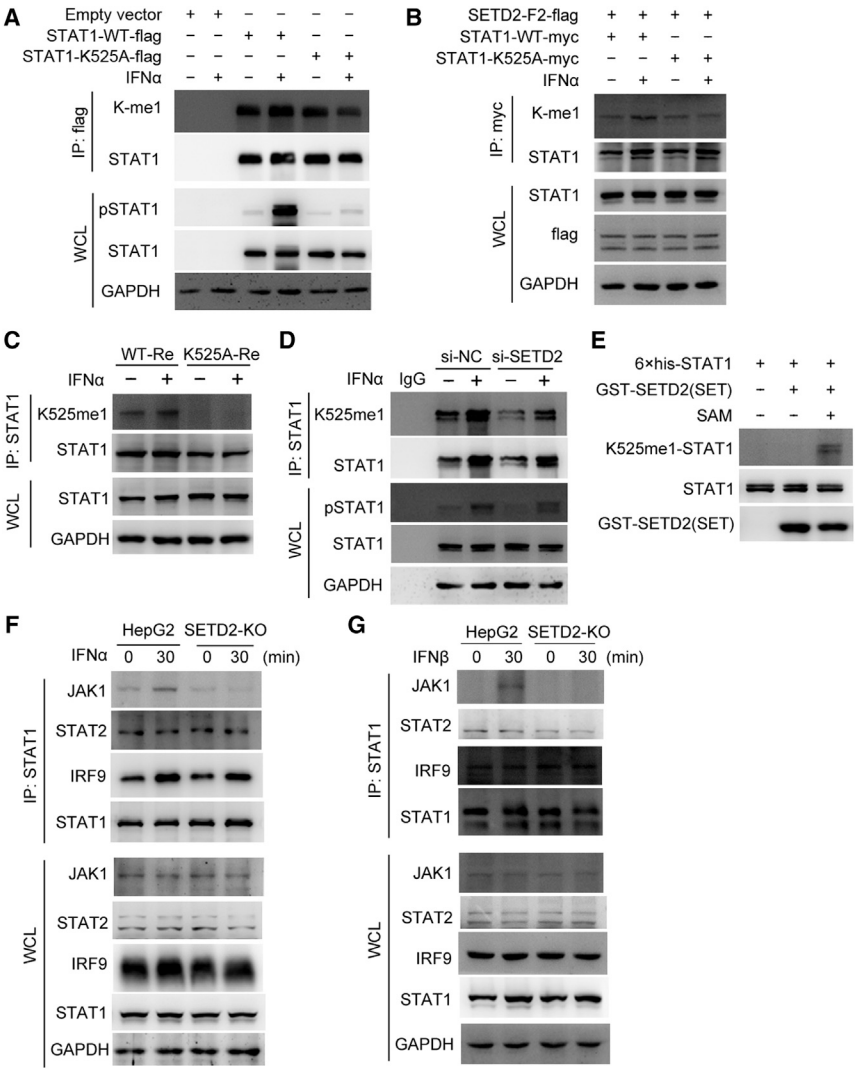

Figure 6. SETD2 Directly Mediates STAT1 K525me1

(A) IB analysis of mono-methylation of STAT1, pSTAT1, total STAT1, and GAPDH in immunoprecipitates, and whole-cell lysates of STAT1-KO cells transfected with flag-tagged STAT1-WT or STAT1-K525A expression plasmids followed by 1,000 U/mL IFNα treatment for 6 hr.

(B) IB analysis of mono-methylation of STAT1 and total STAT1 in immunoprecipitates of STAT1-KO cells co-transfected with flag-tagged SETD2-F2 and myc-tagged STAT1-WT or STAT1-K525A expression plasmids stimulated with IFNα as in (A).

(C) IB analysis of mono-methylation on K525 (K525me1) of STAT1, total STAT1 in immunoprecipitates of STAT1-WT, and STAT1-K525A-rescued STAT1-KO cells stimulated with IFNα as in (A).

(D) IB analysis of STAT1 K525me1, pSTAT1, total STAT1, and GAPDH in immunoprecipitates and the whole-cell lysates of HepG2 cells transfected with si-NC or si-SETD2, stimulated with IFNα as in (A).

(E) IB analysis of STAT1-525me1 in the in vitro methylation assay with purified 6× his-tagged STAT1 and GST-tagged SETD2 truncation (1469–1724 aa) using S-adenosyl-L-methionine (SAM) as the methyl group donor.

(F and G) IB analysis of JAK1, STAT2, IRF9, and STAT1 in immunoprecipitates and the whole-cell lysates of WT and SETD2-KO HepG2 cells treated with IFNα (F) or IFNβ (G) for 30 min.

Data are shown for one representative experiment. Similar results were obtained in three independent experiments. See also Figure S6.

SETD2 Selectively Promotes Expression of ISGs by H3K36me3 Modification

Although the IFNα-induced expression of a set of ISGs such as *ISG15* and *MX2* was reduced by SETD2 silencing (Figure 3I), expression of other ISGs such as *RIG-I* was not affected (data not shown). Thus, SETD2 might regulate expression of ISGs in a gene-selective manner. We therefore performed unbiased transcriptome profiling with RNA-seq in SETD2-KO cells, STAT1-K525A-Re cells, STAT1-KO cells, as well as control HepG2 cells stimulated with IFNα for 6 hr (Figure 7A). Out of the 222 genes that are induced in control HepG2 cells after IFNα stimulation, the induction of 89, 128, and 180 genes was significantly lower in SETD2-KO cells, STAT1-K525A-Re cells, and STAT1-KO cells as compared to that in control HepG2 cells, respectively (Figure 7B). A gene ontology (GO) enrichment analysis demonstrated that the genes with lower expression in SETD2-KO cells and STAT1-K525A-Re cells could be categorized into defense response to virus or type I IFN pathway-related genes (Figure 7C). Among the 180 genes differentially induced in IFNα-stimulated STAT1-KO cells, 40% of them were also lower in IFNα-stimulated SETD2-KO cells, indicating that SETD2 promotes the expression of a set of STAT1-dependent ISG (Figure 7D). In addition, 75 genes showed lower expression both in SETD2-KO cells and STAT1-K525A-Re cells after IFNα stimulation, including those ISGs with potent antiviral functions, such as *ISG15*, *ISG20*, *MX2*, etc. (Figures 7D and 7E). The data further confirmed that SETD2-mediated ISGs regulation is to a large extent dependent on its effect in mediating STAT1 K525 mono-methylation.

Given that SETD2 is the only methyltransferase reported to be required for H3K36me3, a marker of transcriptional activation, we hypothesized that expression of some ISGs are dependent on H3K36me3 modification. By chromatin immunoprecipitation (ChIP)-qPCR assay using anti-H3K36me3 antibody, we found the amount of H3K36me3 in the promoter region of *ISG15* and *IP-10* and the gene body region of *IFIT-1* was increased after IFNα treatment, whereas the amount of H3K36me3 in the promoter region of *RIG-I* remained unchanged. Furthermore, IFNα-induced accumulation of H3K36me3 in the *ISG15* and *IP-10* promoter region and *IFIT-1* gene body region was significantly abolished in both SETD2-silenced and SETD2-KO HepG2 cells, indicating that SETD2 selectively promotes

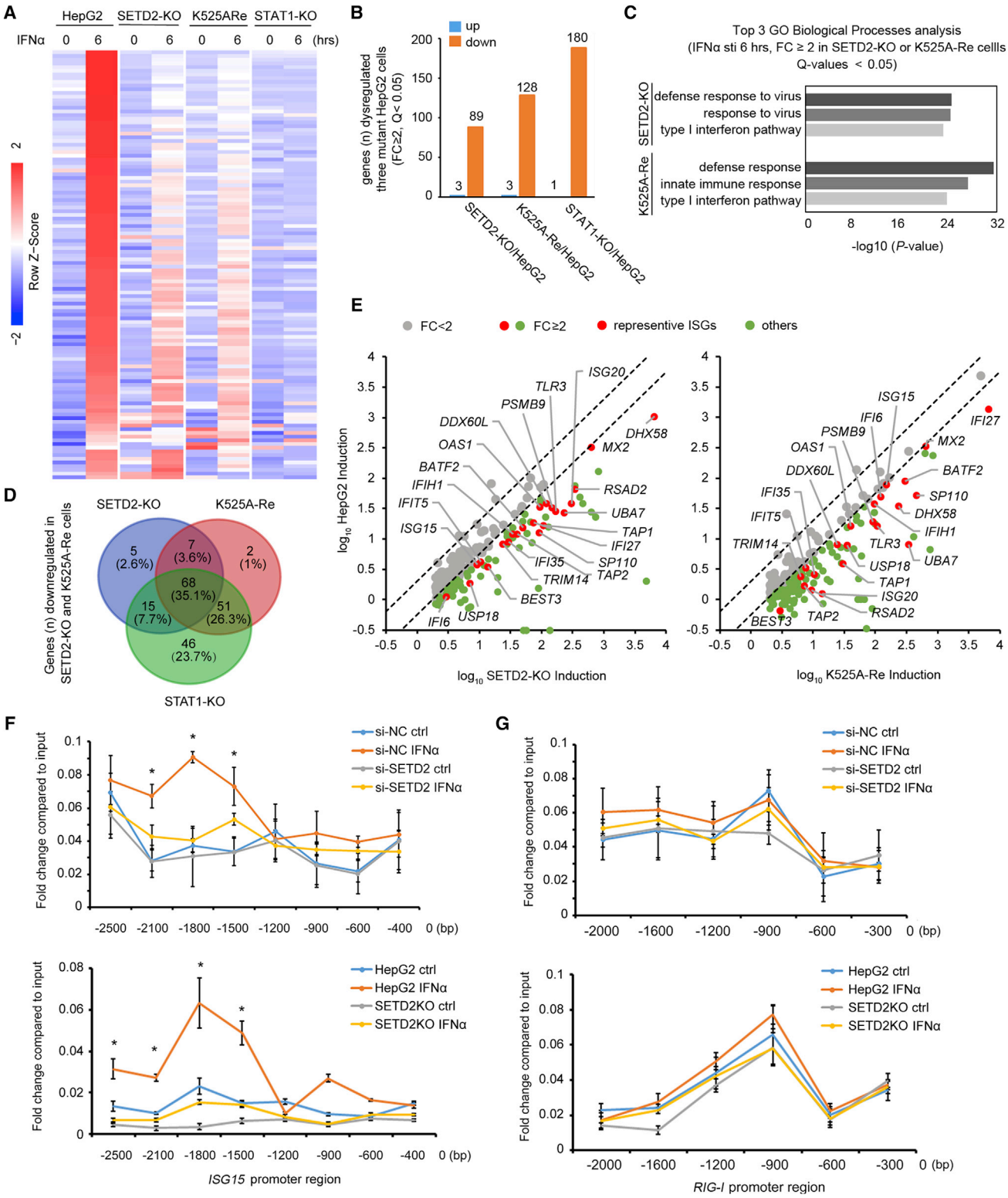

Figure 7. SETD2 Selectively Catalyzes H3K36me3 Modification of Some ISGs

(A) Heatmap of ISGs mRNA expression in HepG2, SETD2-KO, K525A-Re, and STAT1-KO cells with IFNα stimulation for 6 hr.

(B) Statistics of the differentially induced genes in SETD2-KO, K525A-Re, and STAT1-KO HepG2 cells relative to that in control HepG2 cells. Fold change (FC) ≥2, Q value <0.05.

(legend continued on next page)

H3K36me3 in some genes including *ISG15*, *IP-10*, and *IFIT-1* gene loci in response to IFNα (Figures 7F, 7G, S7A, and S7B). Taken together, these data indicate that coordinating with mono-methylating STAT1 on K525 to enhance IFN signaling, SETD2 selectively catalyzes H3K36me3 modification of a set of ISGs gene loci to promote their expression.

DISCUSSION

Identifying how type I IFN-mediated immune response against viruses is activated and tightly regulated has been one of most challenging issues in the field of antiviral innate immunity (Fusco et al., 2013; Pulloor et al., 2014; Schoggins et al., 2011; Zhao et al., 2012). In this study, we performed a high throughput screening of epigenetic modifiers by lentivirus-mediated RNAi to search for the epigenetic factors that are involved in IFNα-mediated antiviral response. This approach yielded the discovery and successfully identified that the methyltransferase SETD2 is a critical effector molecule that increases IFNα-induced STAT1 activation by directly methylating STAT1, opening new avenues for study of the pathogenesis of various immune disorders and outlining potential strategies for disease prevention and treatment. Our screening system can also be broadly applied in a wide variety of biological and immunological investigations, such as cellular responses to inflammatory or cytokine stimuli.

The role of unconventional PTMs, such as acetylation, SUMOylation in regulation of STAT1 activation, and IFN signaling, is attracting more and more attention. It was shown that STAT1 acetylation induced binding of protein tyrosine phosphatase (TCP45) that catalyzes dephosphorylation and inactivation of STAT1 (Ginter et al., 2012). SUMO conjugation of STAT1 is associated with hypo-responsiveness to IFNγ (Begitt et al., 2011). Methylation on Arg31 of STAT1 by protein arginine methyltransferase 1 (PRMT1) is required for IFNα/β-induced gene transcription (Mowen et al., 2001). Here, we identified mono-methylation of STAT1 on lysine 525 as an important PTM that is critical for phosphorylation, nuclear translocation, and DNA-binding activity of STAT1, eventually contributing to IFNα-induced antiviral response. The core region of STAT1 contains four tandem structural domains: coil-coiled domain, DNA binding domain, linker domain, and SH2 domain, and each of the four domains is fused to the adjacent ones by the formation of a contiguous hydrophobic core. Furthermore, interaction between SH2 domain (containing Y701 site for phosphorylation) and the elements of linker domain (containing K525 for methylation) was proposed to be essential for buttressing the phosphate-binding loop of the STAT1 SH2 domain (Chen et al., 1998). Therefore, we propose that SETD2-mediated methylation of STAT1 K525 may promote the formation of phosphate-binding loop in SH2 domain and then facilitate STAT1 Y701 phosphorylation.

SETD2 is responsible for H3K36me3 and has been recently shown to tri-methylate α-tubulin on K40, which is required for mitosis and genomic stability (Park et al., 2016). Here, we discover an important role of SETD2 in promoting IFNα-initiated antiviral immunity via directly mediating K525me1 of STAT1. It will be intriguing to further investigate the crosstalk between histone modification and non-histone PTMs by SETD2 in the context of immunity and inflammation. Interestingly, there was a modest upregulation of HBsAg after overexpression of F3 fragment of SETD2 containing WW domain, indicating a potentially negative regulatory role of the C-terminal fragment of SETD2 in IFNα activity. One possible explanation is that WW domain may have a potential role in affecting antiviral immunity because WW domain of NEDD4 was shown to interact with IFITM3 to inhibit antiviral function (Chesarino et al., 2015).

According to the transcriptional profiling analysis, SETD2 enhances the expression of a set of STAT1-dependent ISG expression. The induction of ISG is a dynamic cellular process significantly dependent on stimulation magnitude, frequency, and time course (Mostafavi et al., 2016). Although SETD2-mediated K525me1 of STAT1 is critical of STAT1 phosphorylation and transcriptional activity, the downstream effect in global ISG expression of SETD2 may be dynamically regulated by other factors such as transcriptional factors, epigenetic enzymes, and chromatin remodelers in the nucleus. Notably, the ISGs dependent on SETD2 and STAT1-K525 methylation include those ones that have been shown to be critical for antiviral responses such as *ISG15*, *ISG20*, *MX2*, etc. Therefore, SETD2-mediated STAT1-K525me1 is essential for the expression of a set of ISGs, consequently contributing to cellular defense against viral infection. It merits further investigation to clarify the mechanism underlying the gene selectivity of SETD2-mediated regulation of ISG expression.

STAR★METHODS

Detailed methods are provided in the online version of this paper and include the following:

- KEY RESOURCES TABLE
- CONTACT FOR REAGENT AND RESOURCE SHARING

(C) Gene ontology (GO) analysis of the differentially expressed genes between SETD2-KO cells or K525A-Re cells and HepG2 cells (FC ≥2 in RNA-seq data) stimulated by IFNα for 6 hr.
(D) Venn diagram of differentially expressed genes (FC ≥2 in RNA-seq data) in SETD2-KO, K525A-Re, and STAT1-KO cells stimulated by IFNα for 6 hr.
(E) Scatterplot diagram of downregulated genes in SETD2-KO cells (left) or K525A-Re cells (right) relative to that in HepG2 cells followed by IFNα treatment. Gray dots represent unchanged expression in both cells, red dots represent the selected ISGs both with lower expression in SETD2-KO and K525A-Re cells, and green dots represent other genes. Dash lines represent 2-fold change.
(F) ChIP analysis of enrichment of H3K36me3 on promoters of *ISG15* in HepG2 cells transfected with si-NC and si-SETD2 or HepG2 WT and HepG2 SETD2-KO cells followed by IFNα treatment.
(G) ChIP analysis of enrichment of H3K36me3 on promoters of *RIG-I* in HepG2 cells transfected with si-NC and si-SETD2 or HepG2 WT and HepG2 SETD2-KO cells treated as in (F).
Data are shown as mean ± SD of three independent experiments (F and G). *$p < 0.05$, **$p < 0.01$. See also Figure S7.

SUPPLEMENTAL INFORMATION

Supplemental Information includes seven figures and three tables and can be found with this article online at http://dx.doi.org/10.1016/j.cell.2017.06.042.

AUTHOR CONTRIBUTIONS

X.C. designed and supervised the research. K.C., J.L., M.X., S.L., X.Z., D.H., Y.J., and C.W. performed research. D.H., Y.J., and C.W. contributed new reagents and analytical tools. K.C., J.L., and X.C. analyzed data and wrote the paper.

ACKNOWLEDGMENTS

We thank Cong Huai for kindly providing plasmids and technical assistance and Lin Yi for the help in animal experiments. This work was supported by the National Natural Science Foundation of China (31390431, 31622024), the National Key Basic Research Program of China (2013CB530503, 2013CB531505), National Mega Projects of China (2017ZX10102032-001), a Mérieux Research Grant (2016), and the CAMS Innovation Fund for Medical Sciences (2016-I2M-1-003).

Received: January 29, 2017
Revised: May 4, 2017
Accepted: June 27, 2017
Published: July 27, 2017

REFERENCES

Begitt, A., Droescher, M., Knobeloch, K.P., and Vinkemeier, U. (2011). SUMO conjugation of STAT1 protects cells from hyperresponsiveness to IFNγ. Blood *118*, 1002–1007.

Biggar, K.K., and Li, S.S. (2015). Non-histone protein methylation as a regulator of cellular signalling and function. Nat. Rev. Mol. Cell Biol. *16*, 5–17.

Cao, X. (2016). Self-regulation and cross-regulation of pattern-recognition receptor signalling in health and disease. Nat. Rev. Immunol. *16*, 35–50.

Carvalho, S., Raposo, A.C., Martins, F.B., Grosso, A.R., Sridhara, S.C., Rino, J., Carmo-Fonseca, M., and de Almeida, S.F. (2013). Histone methyltransferase SETD2 coordinates FACT recruitment with nucleosome dynamics during transcription. Nucleic Acids Res. *41*, 2881–2893.

Carvalho, S., Vítor, A.C., Sridhara, S.C., Martins, F.B., Raposo, A.C., Desterro, J.M., Ferreira, J., and de Almeida, S.F. (2014). SETD2 is required for DNA double-strand break repair and activation of the p53-mediated checkpoint. eLife *3*, e02482.

Chen, T., and Dent, S.Y. (2014). Chromatin modifiers and remodellers: regulators of cellular differentiation. Nat. Rev. Genet. *15*, 93–106.

Chen, X., Vinkemeier, U., Zhao, Y., Jeruzalmi, D., Darnell, J.E., Jr., and Kuriyan, J. (1998). Crystal structure of a tyrosine phosphorylated STAT-1 dimer bound to DNA. Cell *93*, 827–839.

Chen, W., Han, C., Xie, B., Hu, X., Yu, Q., Shi, L., Wang, Q., Li, D., Wang, J., Zheng, P., et al. (2013). Induction of Siglec-G by RNA viruses inhibits the innate immune response by promoting RIG-I degradation. Cell *152*, 467–478.

Cheng, X., Collins, R.E., and Zhang, X. (2005). Structural and sequence motifs of protein (histone) methylation enzymes. Annu. Rev. Biophys. Biomol. Struct. *34*, 267–294.

Cheon, H., and Stark, G.R. (2009). Unphosphorylated STAT1 prolongs the expression of interferon-induced immune regulatory genes. Proc. Natl. Acad. Sci. USA *106*, 9373–9378.

Chesarino, N.M., McMichael, T.M., and Yount, J.S. (2015). E3 ubiquitin ligase NEDD4 promotes influenza virus infection by decreasing levels of the antiviral protein IFITM3. PLoS Pathog. *11*, e1005095.

Dalgliesh, G.L., Furge, K., Greenman, C., Chen, L., Bignell, G., Butler, A., Davies, H., Edkins, S., Hardy, C., Latimer, C., et al. (2010). Systematic sequencing of renal carcinoma reveals inactivation of histone modifying genes. Nature *463*, 360–363.

Dasgupta, M., Dermawan, J.K., Willard, B., and Stark, G.R. (2015). STAT3-driven transcription depends upon the dimethylation of K49 by EZH2. Proc. Natl. Acad. Sci. USA *112*, 3985–3990.

Edmunds, J.W., Mahadevan, L.C., and Clayton, A.L. (2008). Dynamic histone H3 methylation during gene induction: HYPB/Setd2 mediates all H3K36 trimethylation. EMBO J. *27*, 406–420.

Fusco, D.N., Brisac, C., John, S.P., Huang, Y.W., Chin, C.R., Xie, T., Zhao, H., Jilg, N., Zhang, L., Chevaliez, S., et al. (2013). A genetic screen identifies interferon-α effector genes required to suppress hepatitis C virus replication. Gastroenterology *144*, 1438–1449.

Ginter, T., Bier, C., Knauer, S.K., Sughra, K., Hildebrand, D., Münz, T., Liebe, T., Heller, R., Henke, A., Stauber, R.H., et al. (2012). Histone deacetylase inhibitors block IFNγ-induced STAT1 phosphorylation. Cell. Signal. *24*, 1453–1460.

Hou, J., Zhou, Y., Zheng, Y., Fan, J., Zhou, W., Ng, I.O., Sun, H., Qin, L., Qiu, S., Lee, J.M., et al. (2014). Hepatic RIG-I predicts survival and interferon-α therapeutic response in hepatocellular carcinoma. Cancer Cell *25*, 49–63.

Kroetz, D.N., Allen, R.M., Schaller, M.A., Cavallaro, C., Ito, T., and Kunkel, S.L. (2015). Type I interferon induced epigenetic regulation of macrophages suppresses innate and adaptive immunity in acute respiratory viral infection. PLoS Pathog. *11*, e1005338.

Kuzhandaivelu, N., Cong, Y.S., Inouye, C., Yang, W.M., and Seto, E. (1996). XAP2, a novel hepatitis B virus X-associated protein that inhibits X transactivation. Nucleic Acids Res. *24*, 4741–4750.

Langmead, B., and Salzberg, S.L. (2012). Fast gapped-read alignment with Bowtie 2. Nat. Methods *9*, 357–359.

Levy, D., Kuo, A.J., Chang, Y., Schaefer, U., Kitson, C., Cheung, P., Espejo, A., Zee, B.M., Liu, C.L., Tangsombatvisit, S., et al. (2011). Lysine methylation of the NF-κB subunit RelA by SETD6 couples activity of the histone methyltransferase GLP at chromatin to tonic repression of NF-κB signaling. Nat. Immunol. *12*, 29–36.

Li, F., Mao, G., Tong, D., Huang, J., Gu, L., Yang, W., and Li, G.M. (2013). The histone mark H3K36me3 regulates human DNA mismatch repair through its interaction with MutSα. Cell *153*, 590–600.

Li, X., Zhang, Q., Ding, Y., Liu, Y., Zhao, D., Zhao, K., Shen, Q., Liu, X., Zhu, X., Li, N., et al. (2016). Methyltransferase Dnmt3a upregulates HDAC9 to deacetylate the kinase TBK1 for activation of antiviral innate immunity. Nat. Immunol. *17*, 806–815.

Liu, J., Han, C., Xie, B., Wu, Y., Liu, S., Chen, K., Xia, M., Zhang, Y., Song, L., Li, Z., et al. (2014a). Rhbdd3 controls autoimmunity by suppressing the production of IL-6 by dendritic cells via K27-linked ubiquitination of the regulator NEMO. Nat. Immunol. *15*, 612–622.

Liu, Q., Tan, Q., Zheng, Y., Chen, K., Qian, C., Li, N., Wang, Q., and Cao, X. (2014b). Blockade of Fas signaling in breast cancer cells suppresses tumor growth and metastasis via disruption of Fas signaling-initiated cancer-related inflammation. J. Biol. Chem. *289*, 11522–11535.

Liu, J., Qian, C., and Cao, X. (2016). Post-translational modification control of innate immunity. Immunity *45*, 15–30.

Lucifora, J., Xia, Y., Reisinger, F., Zhang, K., Stadler, D., Cheng, X., Sprinzl, M.F., Koppensteiner, H., Makowska, Z., Volz, T., et al. (2014). Specific and nonhepatotoxic degradation of nuclear hepatitis B virus cccDNA. Science *343*, 1221–1228.

Luco, R.F., Pan, Q., Tominaga, K., Blencowe, B.J., Pereira-Smith, O.M., and Misteli, T. (2010). Regulation of alternative splicing by histone modifications. Science *327*, 996–1000.

McNab, F., Mayer-Barber, K., Sher, A., Wack, A., and O'Garra, A. (2015). Type I interferons in infectious disease. Nat. Rev. Immunol. *15*, 87–103.

Mostafavi, S., Yoshida, H., Moodley, D., LeBoité, H., Rothamel, K., Raj, T., Ye, C.J., Chevrier, N., Zhang, S.Y., Feng, T., et al.; Immunological Genome Project Consortium (2016). Parsing the interferon transcriptional network and its disease associations. Cell *164*, 564–578.

Mowen, K.A., and David, M. (2014). Unconventional post-translational modifications in immunological signaling. Nat. Immunol. *15*, 512–520.

Mowen, K.A., Tang, J., Zhu, W., Schurter, B.T., Shuai, K., Herschman, H.R., and David, M. (2001). Arginine methylation of STAT1 modulates IFNalpha/beta-induced transcription. Cell *104*, 731–741.

Ott, J.J., Stevens, G.A., Groeger, J., and Wiersma, S.T. (2012). Global epidemiology of hepatitis B virus infection: new estimates of age-specific HBsAg seroprevalence and endemicity. Vaccine *30*, 2212–2219.

Park, I.Y., Powell, R.T., Tripathi, D.N., Dere, R., Ho, T.H., Blasius, T.L., Chiang, Y.C., Davis, I.J., Fahey, C.C., Hacker, K.E., et al. (2016). Dual chromatin and cytoskeletal remodeling by SETD2. Cell *166*, 950–962.

Pfister, S.X., Ahrabi, S., Zalmas, L.P., Sarkar, S., Aymard, F., Bachrati, C.Z., Helleday, T., Legube, G., La Thangue, N.B., Porter, A.C., and Humphrey, T.C. (2014). SETD2-dependent histone H3K36 trimethylation is required for homologous recombination repair and genome stability. Cell Rep. *7*, 2006–2018.

Pulloor, N.K., Nair, S., McCaffrey, K., Kostic, A.D., Bist, P., Weaver, J.D., Riley, A.M., Tyagi, R., Uchil, P.D., York, J.D., et al. (2014). Human genome-wide RNAi screen identifies an essential role for inositol pyrophosphates in Type-I interferon response. PLoS Pathog. *10*, e1003981.

Rea, S., Eisenhaber, F., O'Carroll, D., Strahl, B.D., Sun, Z.W., Schmid, M., Opravil, S., Mechtler, K., Ponting, C.P., Allis, C.D., and Jenuwein, T. (2000). Regulation of chromatin structure by site-specific histone H3 methyltransferases. Nature *406*, 593–599.

Sadler, A.J., and Williams, B.R. (2008). Interferon-inducible antiviral effectors. Nat. Rev. Immunol. *8*, 559–568.

Scaglione, S.J., and Lok, A.S. (2012). Effectiveness of hepatitis B treatment in clinical practice. Gastroenterology *142*, 1360–1368.

Schneider, W.M., Chevillotte, M.D., and Rice, C.M. (2014). Interferon-stimulated genes: a complex web of host defenses. Annu. Rev. Immunol. *32*, 513–545.

Schoggins, J.W., Wilson, S.J., Panis, M., Murphy, M.Y., Jones, C.T., Bieniasz, P., and Rice, C.M. (2011). A diverse range of gene products are effectors of the type I interferon antiviral response. Nature *472*, 481–485.

Sells, M.A., Chen, M.L., and Acs, G. (1987). Production of hepatitis B virus particles in Hep G2 cells transfected with cloned hepatitis B virus DNA. Proc. Natl. Acad. Sci. USA *84*, 1005–1009.

Stark, G.R., and Darnell, J.E., Jr. (2012). The JAK-STAT pathway at twenty. Immunity *36*, 503–514.

Sun, X.J., Wei, J., Wu, X.Y., Hu, M., Wang, L., Wang, H.H., Zhang, Q.H., Chen, S.J., Huang, Q.H., and Chen, Z. (2005). Identification and characterization of a novel human histone H3 lysine 36-specific methyltransferase. J. Biol. Chem. *280*, 35261–35271.

Sung, P.S., Cheon, H., Cho, C.H., Hong, S.H., Park, D.Y., Seo, H.I., Park, S.H., Yoon, S.K., Stark, G.R., and Shin, E.C. (2015). Roles of unphosphorylated ISGF3 in HCV infection and interferon responsiveness. Proc. Natl. Acad. Sci. USA *112*, 10443–10448.

Xia, M., Liu, J., Wu, X., Liu, S., Li, G., Han, C., Song, L., Li, Z., Wang, Q., Wang, J., et al. (2013). Histone methyltransferase Ash1l suppresses interleukin-6 production and inflammatory autoimmune diseases by inducing the ubiquitin-editing enzyme A20. Immunity *39*, 470–481.

Yan, R., Zhao, X., Cai, D., Liu, Y., Block, T.M., Guo, J.T., and Guo, H. (2015). The interferon-inducible protein tetherin inhibits hepatitis B virus virion secretion. J. Virol. *89*, 9200–9212.

Yang, P.L., Althage, A., Chung, J., and Chisari, F.V. (2002). Hydrodynamic injection of viral DNA: a mouse model of acute hepatitis B virus infection. Proc. Natl. Acad. Sci. USA *99*, 13825–13830.

Yang, S., Zheng, X., Lu, C., Li, G.M., Allis, C.D., and Li, H. (2016). Molecular basis for oncohistone H3 recognition by SETD2 methyltransferase. Genes Dev. *30*, 1611–1616.

Yuan, W., Xie, J., Long, C., Erdjument-Bromage, H., Ding, X., Zheng, Y., Tempst, P., Chen, S., Zhu, B., and Reinberg, D. (2009). Heterogeneous nuclear ribonucleoprotein L Is a subunit of human KMT3a/Set2 complex required for H3 Lys-36 trimethylation activity *in vivo*. J. Biol. Chem. *284*, 15701–15707.

Zhang, J., Ding, L., Holmfeldt, L., Wu, G., Heatley, S.L., Payne-Turner, D., Easton, J., Chen, X., Wang, J., Rusch, M., et al. (2012). The genetic basis of early T-cell precursor acute lymphoblastic leukaemia. Nature *481*, 157–163.

Zhang, Y., Xie, S., Zhou, Y., Xie, Y., Liu, P., Sun, M., Xiao, H., Jin, Y., Sun, X., Chen, Z., et al. (2014). H3K36 histone methyltransferase Setd2 is required for murine embryonic stem cell differentiation toward endoderm. Cell Rep. *8*, 1989–2002.

Zhang, Q., Zhao, K., Shen, Q., Han, Y., Gu, Y., Li, X., Zhao, D., Liu, Y., Wang, C., Zhang, X., et al. (2015a). Tet2 is required to resolve inflammation by recruiting Hdac2 to specifically repress IL-6. Nature *525*, 389–393.

Zhang, Y., Mao, D., Roswit, W.T., Jin, X., Patel, A.C., Patel, D.A., Agapov, E., Wang, Z., Tidwell, R.M., Atkinson, J.J., et al. (2015b). PARP9-DTX3L ubiquitin ligase targets host histone H2BJ and viral 3C protease to enhance interferon signaling and control viral infection. Nat. Immunol. *16*, 1215–1227.

Zhao, H., Lin, W., Kumthip, K., Cheng, D., Fusco, D.N., Hofmann, O., Jilg, N., Tai, A.W., Goto, K., Zhang, L., et al. (2012). A functional genomic screen reveals novel host genes that mediate interferon-alpha's effects against hepatitis C virus. J. Hepatol. *56*, 326–333.

Zhu, X., He, F., Zeng, H., Ling, S., Chen, A., Wang, Y., Yan, X., Wei, W., Pang, Y., Cheng, H., et al. (2014). Identification of functional cooperative mutations of SETD2 in human acute leukemia. Nat. Genet. *46*, 287–293.

STAR★METHODS

KEY RESOURCES TABLE

REAGENT or RESOURCE	SOURCE	IDENTIFIER
Antibodies		
anti-pSTAT1	Cell Signaling Technology	Cat #9171; RRID: AB_331591
anti-STAT1	Cell Signaling Technology	Cat #9172; RRID: AB_10831362
anti-flag	Cell Signaling Technology	Cat #2368; RRID: AB_2217020
anti-IRF9	Cell Signaling Technology	Cat #76684
anti- GST	Cell Signaling Technology	Cat #2625; RRID: AB_490796
anti-histone 3	Abcam	Cat #ab1971
anti-H3K36me3	Abcam	Cat #ab9050; RRID: AB_306966
anti-lamin A/C	Abcam	Cat #ab108595; RRID: AB_10866185
anti- HBcAg	Abcam	Cat #ab115992; RRID: AB_10903422
anti-GAPDH	Proteintech	Cat #HRP-60004
anti-STAT2	Millipore	Cat #07-140; RRID: AB_11213767
anti-pSTAT2	Millipore	Cat #07-224; RRID: AB_2198439
anti-K525me1	ABmart	Cat #26703-1hV
anti-SETD2	Abclonal	Cat #A3194
FITC-conjugated anti-mouse IgG antibody	BD Bioscience	Cat #555988; RRID: AB_396275
Bacterial and Virus Strains		
DH5α	Transgen Biotech	Cat #CD201
Rosetta	Tiangen Biotech	Cat #CB108
Chemicals, Peptides, and Recombinant Proteins		
Human Interferon Alpha 2 (Alpha 2b)	Pestka Biomedical Laboratories	Cat #11105-1
Mouse Interferon Alpha A	Pestka Biomedical Laboratories	Cat #12100-1
Recombinant Human IFN-β	PeproTech	Cat #300-02BC
Recombinant Human IFN-γ	PeproTech	Cat #300-02
Recombinant Human IFN-λ1	PeproTech	Cat #300-02L
Recombinant Human M-CSF	PeproTech	Cat # 300-25
APC-conjugated Annexin V	BD Bioscience	Cat # 550474
propidium iodide	BD Bioscience	Cat # 556463
Critical Commercial Assays		
human HBsAg ELISA kit	Kehua Biotechnology (http://www.skhb.com/cn/)	Cat # S10910113
GST Protein Interaction Pull-Down Kit	Thermo	Cat # 21516
LightShift EMSA Optimization and Control Kit	Thermo	Cat # 20148X
ChIP assay kit	Millipore	Cat # 17-371FR
Deposited Data		
RNA-seq raw data	This paper	GEO: GSE98372
Experimental Models: Cell Lines		
HepG2	Cell Bank of the Chinese Academy of Sciences	N/A
HepG2.2.15	Cell Bank of the Chinese Academy of Sciences	N/A
BHK-21	ATCC	Cat # CCL-10
HEK293t	ATCC	Cat # CRL-11268

(*Continued on next page*)

Continued

REAGENT or RESOURCE	SOURCE	IDENTIFIER
BEL-7402	Cell Bank of the Chinese Academy of Sciences	N/A
SETD2-knockout HepG2	This paper	N/A
STAT1-knockout HepG2	This paper	N/A
Experimental Models: Organisms/Strains		
Ifnar1 deficient (*Ifnar1*$^{-/-}$) C57BL/6 mice (B6.129S2-*Ifnar1*^{tm1Agt})	The Jackson Laboratory	JAX stock 010830
Alb-cre mice (B6.Cg-Tg(Alb-cre)21Mgn/J)	The Jackson Laboratory	JAX stock 003574
Setd2$^{fl/fl}$ mice	This paper	N/A
Oligonucleotides		
siRNA: SETD2: 5′- GCUCAGAGUUAACGUUUGA-3′ (sense)	Genepharma	N/A
siRNA: scrambled control RNA: 5′-UUCUCCGAAC GUGUCACGUTT-3′ (sense)	Genepharma	N/A
Primer: *hACTINB* (Fw): 5′-AGAAGGATTCCTAT GTGGGCG-3′	This paper	N/A
Primer: *hACTINB* (Rev): 5′-GGATAGCACAGCCT GGATAGCA-3′	This paper	N/A
Primer: *hISG15* (Fw): 5′- GGACAAATGCGACGA ACC-3′	This paper	N/A
Primer: *hISG15* (Rev): 5′- CCCGCTCACTTGCT GCTT-3′	This paper	N/A
Primer: *hMX2* (Fw): 5′- TCATCAGCCTGGAGAT CACC-3′	This paper	N/A
Primer: *hMX2* (Rev): 5′- CCACCACCAAGTTG ATCGTC-3′	This paper	N/A
Primer: *mActinb* (Fw): 5′- AGTGTGACGTTGACA TCCGT-3′	This paper	N/A
Primer: *mActinb* (Rev): 5′- GCAGCTCAGTAACAG TCCGC-3′	This paper	N/A
Primer: *mIsg15* (Fw): 5′- CGGGAACAAGTCCA CGAAG-3′	This paper	N/A
Primer: *mIsg15* (Rev): 5′- CCCTCAGGCGCAA ATGCT-3′	This paper	N/A
Recombinant DNA		
Plasmid: pcDNA3.1(-)	Invitrogen	Cat # V795-20
Plasmid: pcDNA3.1-myc	Invitrogen	Cat # V855-20
Plasmid: pcDNA3.1-flag	This paper	N/A
Plasmid: pcDNA3.1-SETD2-fragment1-flag	This paper	N/A
Plasmid: pcDNA3.1-SETD2-fragment2-flag	This paper	N/A
Plasmid: pcDNA3.1-SETD2-fragment3-flag	This paper	N/A
Plasmid: pcDNA3.1-ASH1L-fragment3 (SET domain containing)	Xia et al., 2013	N/A
Plasmid: pGEX-2T	GE Life Sciences	Cat # 28-9546-53
Plasmid: pET-28a-6 × His	Novagen	Cat # 69864-3
Probe: ISRE Forward: 5′-GGG AAA GGG AAA CCG AAA CTG A-3′	Sangon Biotechology	N/A
Probe: ISRE Reverse: 5′-TTC AGT TTC GGT TTC CCT TTC CC-3′	Sangon Biotechology	N/A
Probe: GAS Forward: 5′-CGA CAT TTC CCG TAA ATC TG-3′	Sangon Biotechology	N/A

(*Continued on next page*)

Continued

REAGENT or RESOURCE	SOURCE	IDENTIFIER
Probe: GAS Reverse: 5′-CAG ATT TAC GGG AAA TGT CG-3′	Sangon Biotechology	N/A
Software and Algorithms		
Leica laser scanning software	Leica	http://www.leica-microsystems.com/products/confocal-microscopes/details/product/leica-tcs-sp8/
FACSDiva software	BD Bioscience	http://www.bdbiosciences.com/br/instruments/software/facsdiva/resources/overview.jsp
Bowtie2	Langmead and Salzberg, 2012	http://bowtie-bio.sourceforge.net/index.shtml
Other		
Ni HiTrap Chelating High Performance column	GE Life Sciences	Cat # 17-5248-01
AKTAprime	GE Life Sciences	Cat # 11001313

CONTACT FOR REAGENT AND RESOURCE SHARING

Further information and requests for resources and reagents should be directed to and will be fulfilled by the Lead Contact, Xuetao Cao (caoxt@immunol.org).

EXPERIMENTAL MODEL AND SUBJECT DETAILS

Mice

Ifnar1 deficient (*Ifnar1*$^{-/-}$) C57BL/6 mice (B6.129S2-*Ifnar1*^{tm1Agt}) and Alb-cre mice (B6.Cg-Tg(Alb-cre)21Mgn/J) were obtained from The Jackson Laboratory. C57BL/6 mice (6-8 weeks of age) were obtained from the Shanghai Laboratory Animal Center, Chinese Academy of Science. *Setd2*$^{fl/fl}$ mice were generated by Bacterial Artificial Chromosomes (BAC) recombineering technology. Shortly, by homologous recombination, two *floxp* sequences were inserted and located at the upstream and downstream intron of the 3rd exon of *Setd2* gene in mice embryonic stem cell (ES) clones, respectively. Then ES clones with *floxp* were injected into C57BL/6 blastocysts to generate high-percentage chimeras. *Setd2*-floxed allele (*Setd2*$^{fl/fl}$) crossing with Alb-cre^{+} mice generated *Setd2* conditional knockout mice (*Setd2*$^{fl/fl}$ Alb-cre^{+}). All mice were maintained in SPF conditions. All animal experiments were performed according to the National Institute of Health Guide for the Care and Use of Laboratory Animals, with the approval of the Scientific Investigation Board of Second Military Medical University, Shanghai.

Clinical Specimens

The liver tissue samples of HCC and adjacent tissues were obtained from 30 HCC patients who underwent open surgery in 2015 at Shanghai Eastern Hepatobiliary Surgery Hospital. Normal human liver tissues were obtained from distal normal liver tissue of 6 liver hemangioma patients (with no history of HBV infection) from Shanghai Changzheng Hospital. Liver tissue samples were immediately snap frozen in liquid nitrogen and then stored at −80°C as described previously (Hou et al., 2014). Donors were all male patients on average 55 years old (range from 35-70 years old). All samples were collected with written informed consent from the patients and were approved by the institutional review board at each study center.

Culture and Maintenance of Cells

HEK293T and BHK-21 cell lines were from American Type Culture Collection; HepG2.2.15 cell line was from Cell Bank of the Chinese Academy of Sciences; Hepatocellular carcinoma (HCC) cell lines HepG2 and BEL-7402 were obtained as reported previously (Hou et al., 2014). Primary mouse hepatocytes were isolated from mouse liver tissue digested by IV Collagenase. Above cell lines were maintained in endotoxin-free DMEM (PAA laboratory), supplemented with 10% FCS (GIBCO), 5 mg/ml penicillin (GIBCO) and 10 mg/ml streptomycin (GIBCO), at 37°C with 5% CO_2.

Human peripheral blood mononuclear cells (PBMNCs) were collected and purified by Ficoll-Paque PLUS (GE healthcare) density gradient centrifugation. Human CD14+ monocytes were then purified from human PBMCs by CD14^{+} Cell Isolation Kit (Miltenyi Biotec, CA, USA) and then cultured for 6 days in RPMI-1640 supplemented with 10% FCS (GIBCO) and 10 ng/ml hM-CSF (Perprotech) for generation of human macrophages.

METHOD DETAILS

Generation and Validation of SETD2/STAT1 Knockout Cells

Three gRNAs were designed to knock out *SETD2* (5′- CCG CAG CCG CCT CCG AAG AT −3′ (to target *SETD2* exon1), 5′- AAT GAA CTG GGA TTC CGA CG −3′ (to *SETD2* exon3) and 5′- TGC GGA TCA GCC AAT TGC CG −3′ (to *SETD2* exon9)). One sgRNA was picked to knock out *STAT1* (5′- AGG TCA TGA AAA CGG ATG G −3′).

To validate and pick out the knockout cell colonies, genomic DNA was extracted from the parental and knockout HepG2 cells and amplified with primers located ~300 bp from the target site. PCR products were Sanger sequenced, and sequences were aligned using the BioEdit ClustalW multiple sequence alignment tool.

High Throughput Screening

A lentivirus library of 1422 unique shRNAs targeting 711 human epigenetic modifiers (3D-HTS Technology) was used in the high throughput screening (Table S1). In the primary screening, 1×10^3 HepG2.2.15 cells were seeded in each well of 96-well plates and infected by the arrayed one single and distinct lentivirus. 72 hr after infection, cells were treated with 1,000 U/ml human IFNα-2b (Pestka Biomedical Laboratories) for another 12 hr. The supernatants were harvested and assessed for the secreted HBsAg concentration by ELISA. The fold changes of HBsAg secretion of lentivirus-transfected HepG2.2.15 cells were normalized to the scrambled shRNA. In the secondary screening, three individual siRNAs were designed and synthesized for each candidate, transfected into the seeded HepG2.215 cells, and treated as in primary screen. Genes were regarded as positive hits if they were scored by at least two siRNAs.

Generation of SETD2-KO Cells or STAT1-KO Cells

The SETD2 or STAT1 knockout (KO) cells were constructed using the CRISPR/Cas9 gene-editing system. The CRISPR plasmid, a kind gift from Dr. Cong Huai (Fudan University), contains expression cassettes of Cas9, chimeric gRNA and CopGFP. The target sequences of gRNAs were designed using the MIT online tool (http://crispr.mit.edu/), and are listed in STAR Methods. The CRISPR plasmids were transfected into HepG2 cells using JET-PEI (Polyplus-transfection), and single-cell colonies of GFP-positive cells were picked and validated at DNA and protein expression level by genomic DNA sequencing and western blot.

Generation of the Mouse Model of HBV Acute Infection

The HBV acute infection mouse model was generated by HTV injection of the plasmids pHBV1.3, which contain a replication-competent 1.3-fold over-length type C HBV genome. In brief, 20 μg of pHBV 1.3 plasmids solution were diluted into 1.5 mL saline (final volume), and were injected into tail vein of mice within 5-7 s for maximum liver absorption (Yang et al., 2002). The control group received 1.5 mL saline without any plasmids. Sera were harvested at indicated time after injection from the whole blood of mice. The concentration of aspartate aminotransferase (AST), alanine aminotransferase (ALT) and HBsAg level were measured by ELISA.

Mass Spectrometry (MS) Analysis of Lysine Methylation

MS analysis was performed as described (Li et al., 2016). In brief, 1×10^8 HepG2 cells were treated with 1,000 U/ml IFNα for 6 hr, and then lysed in 6 mL M-PER Protein Extraction buffer. Extracts was subjected to immunoprecipitation with 10 μg antibody specifically recognizing STAT1 (Cell Signaling Technology) or IgG overnight at 4°C. Then pre-blocked 100 μL protein A/G agarose beads with 0.1% BSA were added to incubation for 2 hr. Beads were washed three times with NETN (100 mM NaCl, 20 mM Tris-HCl (pH 8.0), 1 mM EDTA, 0.05% (v/v) NP-40), then boiled and loaded to SDS-PAGE. After Coomassie Blue staining, the STAT1 specific bands compared to IgG control were cut and then analyzed in reverse-phase nanospray liquid chromatography–tandem mass spectrometry. The spectra from tandem mass spectrometry were automatically used for searching against the non-redundant International Protein Index mouse protein database (version 3.72) with the Bioworks browser (rev.3.1).

RNA Interference

siRNAs were transfected using INTERFERin (Polyplus-transfection) at a final concentration of 20 nM following manufacturer's instructions.

Cell Growth Assay

Cell growth of HCC cell lines was determined using Cell Counting Kit-8 (CCK8) (Dojindo) according to manufacturer's protocol. Briefly, 1×10^3 cells were seeded into 96-well plates and transfected with siRNAs; 36 hr after transfection, fresh culture medium with 10 μL CCK8 solution was added and incubated for 1 hr at 37°C. The absorbance was measured at 450 nm.

RNA Isolation and qRT-PCR Assay

Total RNA was extracted from cells and frozen human liver tissues using TRIzol reagent (Invitrogen) according to manufacturer's protocol. qRT-PCR analysis was performed using LightCycler (Roche) and SYBR RT-PCR kit (Takara) as described previously (Liu et al., 2014a). Data were normalized to GAPDH expression.

Viral Infection and TCID50 Assay

Cells were infected with VSV, HSV and VACV (1 MOI) for 24 hr. Then the supernatants collected for $TCID_{50}$ assay as described previously (Chen et al., 2013).

Flow Cytometry

Apoptosis analysis was performed by flow cytometry as previously described (Hou et al., 2014). Briefly, cells were treated with 1,000 U/ml human IFNα-2b for the indicated time, harvested, washed, and stained with Annexin V-APC and propidium iodide (PI) at room temperature for 15 min. Resuspended cells were subjected to FACS analysis using a LSR II and data were analyzed by FACSDiva software (BD Biosciences).

ELISA

Secreted HBsAg in cell culture supernatants or sera from acute HBV mouse model were analyzed using human HBsAg ELISA kit (Shanghai Kehua Bio-engineering Co., Ltd) following the manufacturer's instructions. Levels of alanine transaminase (ALT) and aspartate transaminase (AST) in serum of mice were detected using ELISA kits (Rongsheng) following the manufacturer's protocol.

Immunoprecipitation and Western Blot

Cells were harvested and lysed using M-PER Protein Extraction Reagent (Pierce), nuclear extracts from cells were prepared using NE-PER Nuclear and Cytoplasmic Extraction Reagents (Thermo Fisher) following manufacturer's instructions supplemented with protease inhibitor cocktail (Calbiochem). Protein concentrations were determined with bicinchoninic acid assay (Pierce). Equalized extracts were used for immunoprecipitation and immunoblot analysis, which has been described previously (Chen et al., 2013).

Electrophoretic Mobility-Shift Assay

Wild-type and K525A STAT1 plasmid-transfected cells were stimulated by IFNα. These cells were lysed and then incubated with biotin-labeled ISRE (Forward: 5′-GGG AAA GGG AAA CCG AAA CTG A-3′, reverse: 5′-TTC AGT TTC GGT TTC CCT TTC CC-3′) and GAS (Forward: 5′-CGA CAT TTC CCG TAA ATC TG-3′, reverse: 5′-CAG ATT TAC GGG AAA TGT CG-3′) probe (Synthesized by Sangon Biotechology) before being separated by electrophoresis and visualized by autoradiography.

Expression and Purification of GST or 6 × His Fusion Proteins and Histone Proteins Extraction

The sequence encoding STAT1 was cloned into a pET-28a expression vector between the NheI and NotI sites, followed by a 6 × his tag. Sequences encoding SETD2 truncated fragments were cloned into pGEX-2T expression vectors between BamHI and EcoRI sites. STAT1 and SETD2 truncation expression vectors were transformed into *Rosetta E. coli* strain, then induced with 0.5 mM isopropy-β-D-thiogalactoside (IPTG) (Sigma-Aldrich) at 20°C for 20 hr.

The expressed STAT1 proteins were purified using a 5 mL Ni HiTrap Chelating High Performance column (GE Life Sciences) with an AKTAprime plus system (GE Life Sciences), and then dialysed and stored in TBS buffer (25 mM Tris-HCl, 0.15 M NaCl, pH 7.2) at −80°C.

The SETD2 truncated proteins were generated as follows: T1 (1∼402 amino acids (aa.) of human SETD2), T2 (451∼1067 aa.), T3 (1061∼1691 aa.), T3N (962∼1345 aa.), T3C (1252∼1691 aa.), T4N (1469-1724 aa.), T4C (1704∼2076 aa.), T4 (1389∼2021 aa.), T5 (1940∼2284 aa.) and T6 (2084∼2564 aa.) truncated fragments tagged with GST were transformed into *Rosetta E. coli* strain and induced with 0.5 mM IPTG. Cells were collected and lysed in a high pressure cell disruptor (Constant Systems), and the expressed proteins were purified using the GST Spin Purification Kit (Pierce) following the manufacturer's instruction. In brief, protein extracts were incubated with resin bed containing Glutathione agarose, washed with Tris buffer (125 mM Tris, 150 mM sodium chloride, pH 8.0) five times, and GST-tagged proteins were eluted from the resin with Elution Buffer (3 mg/ml Glutathione in 125 mM Tris, 150 mM sodium chloride buffer.)

Histone proteins were extracted from 1×10^7 HepG2 cells following the histone extraction protocol available online (http://www.abcam.com/protocols/histoneextraction-protocol-for-western-blot). Briefly, cells were lysed in Triton Extraction Buffer (TEB: PBS with 0.5% Triton X-100 (v/v) and protease inhibitor cocktail) on ice for 15 min. The pellet was then incubated in 0.2N HCl buffer overnight at 4°C, and the supernatant was collected after centrifugation.

GST Pull-down Assay

GST pull-down assays were performed using GST Protein Interaction Pull-Down Kit (Pierce) following the manufacturer's instruction. In brief, 800 μg purified STAT1 protein was incubated with 100 μg of GST-tagged SETD2 truncated proteins or GST control protein in TBS buffer with glutathione agarose beads overnight at 4°C. The incubated proteins were then washed and immunoblotted using anti-STAT1 antibody.

In Vitro Methylation Assay

30 ng/μl purified SETD2 truncated fragment (1469-1724 aa.) and 30 ng/μl purified STAT1 or histone proteins were incubated in the reaction buffer with protease inhibitor cocktail (Merck) overnight at room temperature. The reaction buffer contained 50 mM Tris-HCl (pH 8.0), 2 mM $MgCl_2$, 0.01% Trion X-100 (Takara), 1 mM Tris (2-CarboxyEthyl) Phosphine (TCEP) (Hampton Research) and 0.5 mM SAM (New England Biolabs) as the methyl group donor.

Immunofluorescence

Paraffin-embedded sections of liver biopsies were performed as described (Liu et al., 2014b). Briefly, liver biopsies were fixed, embedded into paraffin blocks, dewaxed, rehydrated, and microwaved. Sections were labeled with mouse anti-HBcAg (Abcam) and then FITC-conjugated to anti-mouse IgG antibody. The intracellular distributions of HBcAg were observed by confocal microscope and the Leica laser scanning software (TCS-SP2).

RNA-seq Analysis

Total RNA was isolated and used for RNA-seq analysis. cDNA library construction and sequencing were performed by Beijing Genomics Institute using BGISEQ-500 platform. High-quality reads were aligned to the human reference genome (GRCh38) using Bowtie2. The expression levels for each of the genes were normalized to fragments per kilobase of exon model per million mapped reads (FPKM) using RNA-seq by Expectation Maximization (RSEM).

Chromatin Immunoprecipitation (ChIP) Analysis

ChIP analysis was performed as described (Zhang et al., 2015a) with H3K36me3 (ab9050) and the assay was performed according to manufacturer's instructions of the ChIP assay kit (Millipore). Fold enrichment was quantified using qRT-PCR and calculated as a percentage of input chromatin (% input).

QUANTIFICATION AND STATISTICAL ANALYSIS

The statistical significance of comparisons between two groups was analyzed with Student's t test. Differences were considered to be statistically significant when p values were less than 0.05.

DATA AND SOFTWARE AVAILABILITY

The RNA-seq data in this paper have been deposited in the Gene Expression Omnibus (GEO) with accession number GSE98372.

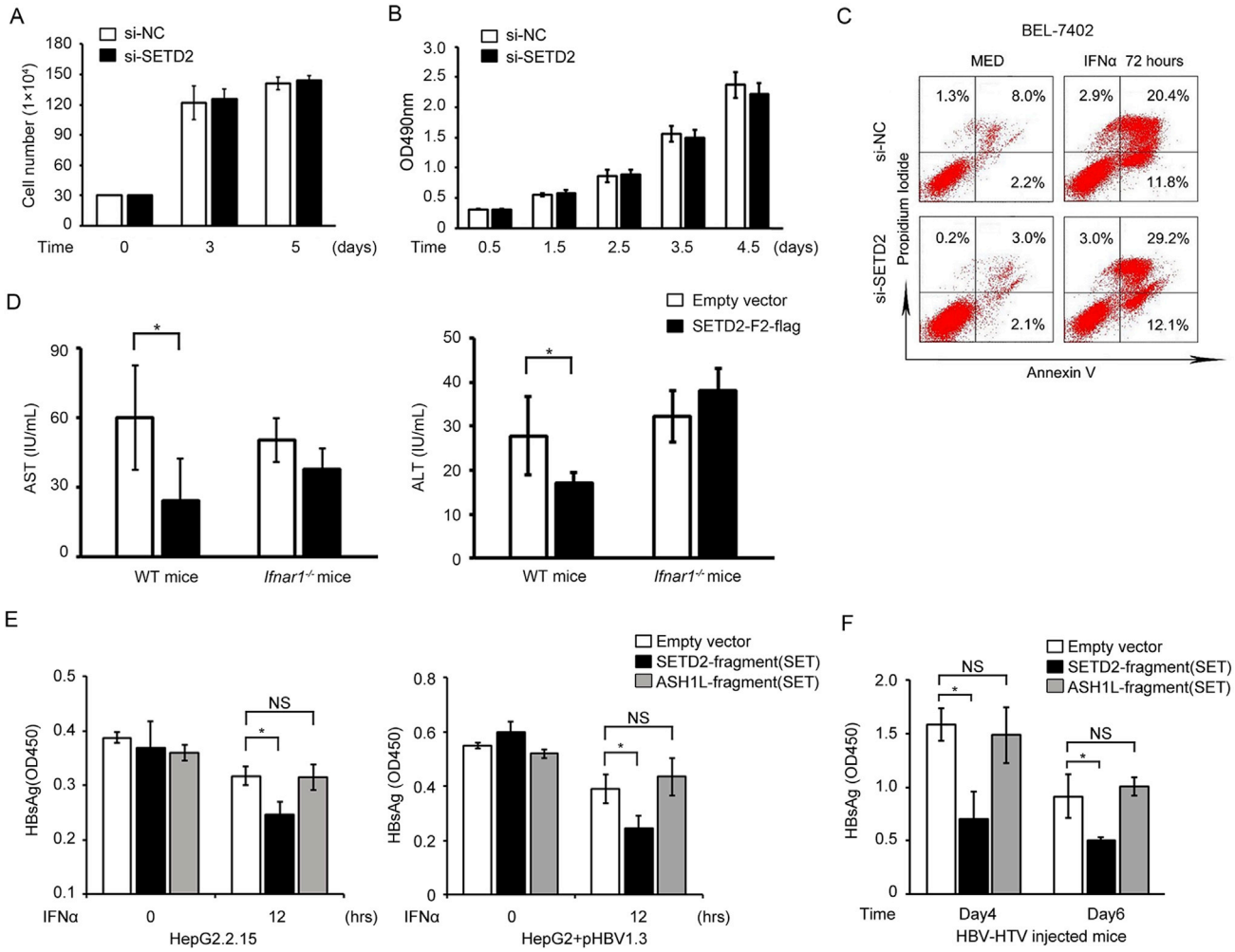

Figure S1. SETD2 Prevents Liver Injury in HBV-Injected Mice via SET Domain-Containing Fragment, Related to Figure 2

(A and B) Proliferation of HepG2 cells transfected with si-NC and si-SETD2 at indicated times as measured by direct cell counting and CCK8 assay.

(C) Flow cytometry of HCC cells transfected as in (A) followed by 1,000 U/ml IFNα treatment for 72 hr. Data are shown for one representative experiment.

(D) ELISA of AST and ALT in sera from WT or *Ifnar1*$^{-/-}$ mice after HTV injection with pHBV1.3 and empty vector or flag-tagged SETD2-F2 expression plasmids.

(E) ELISA of supernatant HBsAg from HepG2.2.15 transfected with empty vector, flag-tagged SETD2-F2 or flag-tagged Ash1l-fragment (SET) expression plasmid (left) and HepG2 co-transfected with pHBV1.3 and empty vector, flag-tagged SETD2-F2 or flag-tagged Ash1l-fragment (SET) expression plasmids (right) followed by 1,000 U/ml IFNα treatment for the indicated time.

(F) ELISA of serum HBsAg in mice at indicated time after HTV-injection with pHBV1.3 or flag-tagged SETD2-F2 or flag-tagged Ash1l-fragment (SET) expression plasmids. Data are shown as mean ± s.d. (n = 6). *$p < 0.05$, NS, not significant.

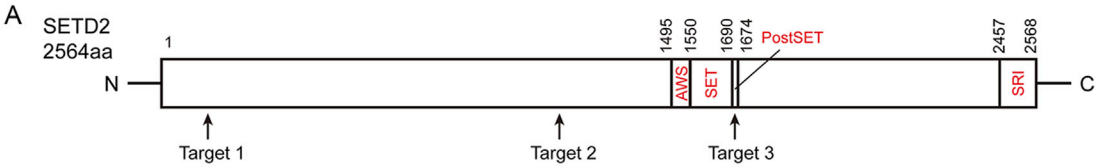

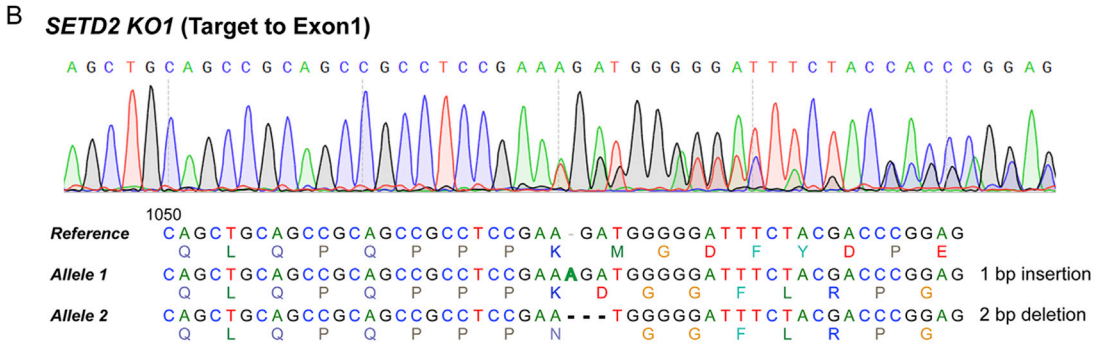

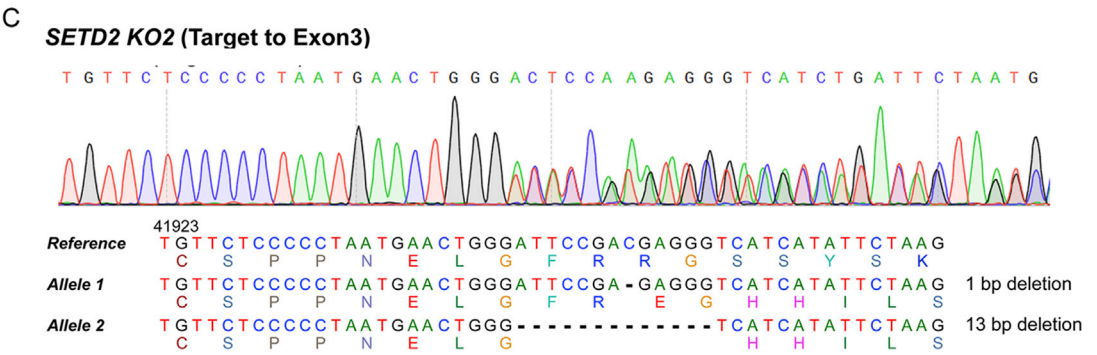

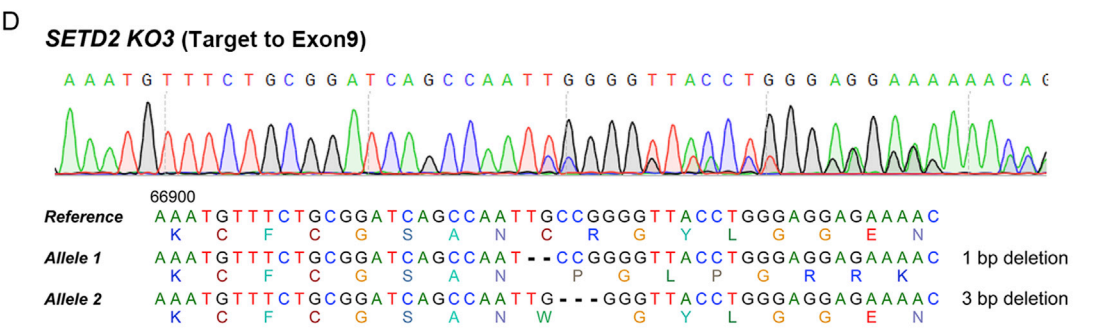

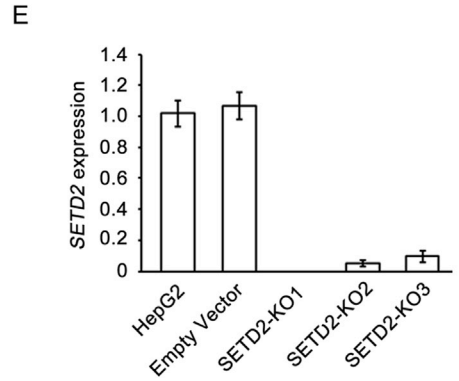

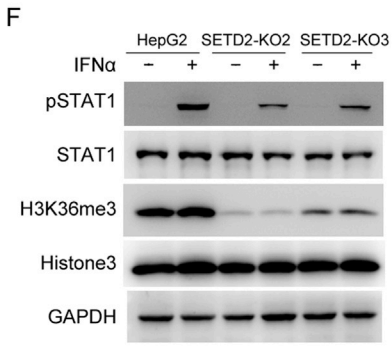

(legend on next page)

Figure S2. Generation of SETD2 Knockout HepG2 Cell Lines, Related to Figure 2

(A) Schematic diagram showing full-length SETD2 protein and the target sites used for CRISPR/Cas9 gRNA design.

(B–D) Sanger-sequencing analysis of genomic DNA from SETD2-knockout (KO) cells. The sequencing results indicate the formation of frameshift mutations in the shown three KO cells lines.

(E) qRT-PCR analysis of *SETD2* expression in WT and SETD2-KO HepG2 cells.

(F) Immunoblot analysis of pSTAT1, STAT1, H3K36me3, Histone3 and GAPDH in the whole-cell lysates of control, SETD2-KO2 and SETD2-KO3 HepG2 cells treated with 1,000 U/ml IFNα for 1 hr.

Data are representative of three independent experiments with similar results or shown as mean ± s.d. of three independent experiments (E). *$p < 0.05$, **$p < 0.01$.

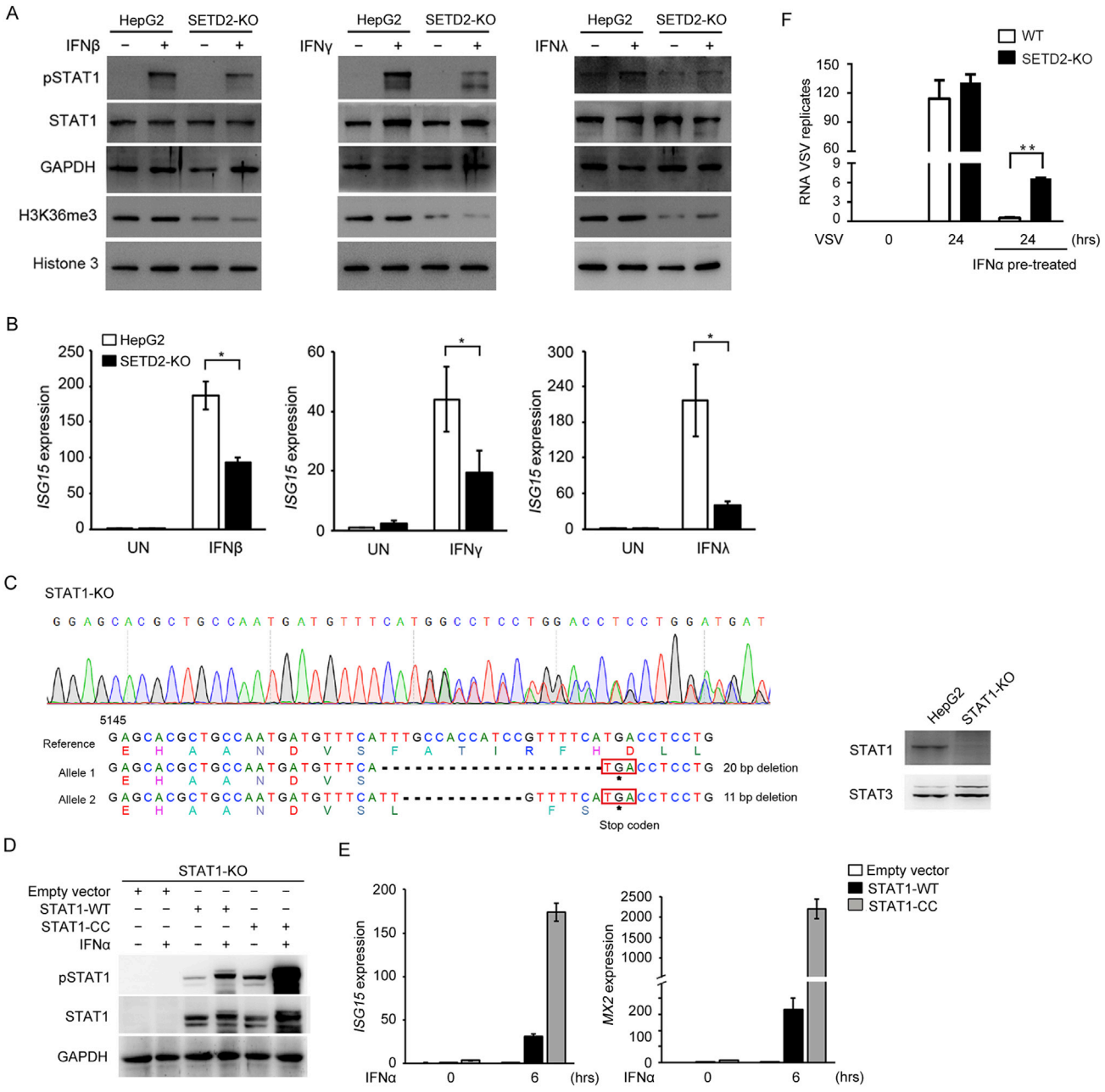

Figure S3. SETD2 Facilitates IFNα-Induced STAT1 Phosphorylation, Related to Figure 3

(A) IB analysis of pSTAT1, STAT1, H3K36me3, Histone3 and GAPDH in the whole-cell lysates of control and SETD2-KO cells treated with 100 ng/ml IFNβ, IFNγ and IFNλ for 6 hr.

(B) qRT-PCR analysis of *ISG15* expression in control and SETD2-KO HepG2 cells stimulated as in (A).

(C) Sanger-sequencing analysis of genomic DNA from STAT1-KO cells generated using CRISPR/Cas9 technology. The sequencing result indicates the formation of frameshift mutations in STAT1-KO cell line (left). IB analysis of STAT1 and STAT3 in control and STAT1-KO HepG2 cells (right).

(D) IB analysis of pSTAT1, STAT1 and GAPDH in whole-cell lysates of STAT1-KO cells transfected with STAT1-WT and STAT1-CC expression plasmids and stimulated with IFNα.

(E) qRT-PCR analysis of *ISG15* and *MX2* expression in STAT1-KO cells transfected and stimulated as in (D).

(F) qRT-PCR analysis of VSV in control and SETD2-KO HepG2 cells pre-treated with 1,000 U/ml IFNα or medium alone for 12 hr and then infected by VSV for 24 hr. Data are representative of three independent experiments with similar results or shown as mean ± s.d. of three independent experiments (B, E and F). *$p < 0.05$, **$p < 0.01$.

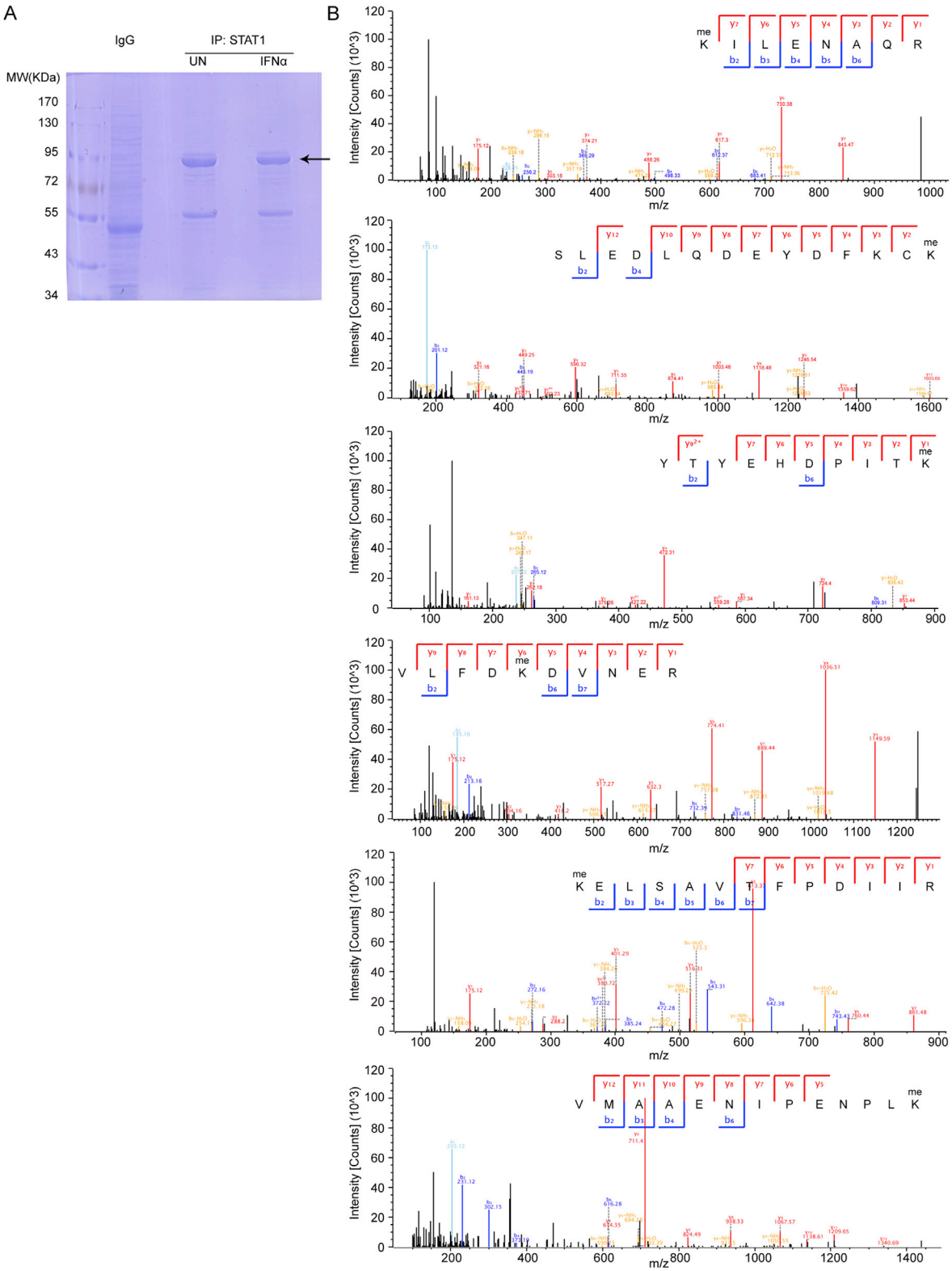

Figure S4. SETD2 Induces Mono-methylation of STAT1 via Methyltransferase Activity of Its SET Domain, Related to Figure 5

(A) SDS-PAGE of purified proteins immunoprecipitated by anti-STAT1 antibody.

(B) MS analysis of STAT1-specific bind cut from SDS-PAGE gel.

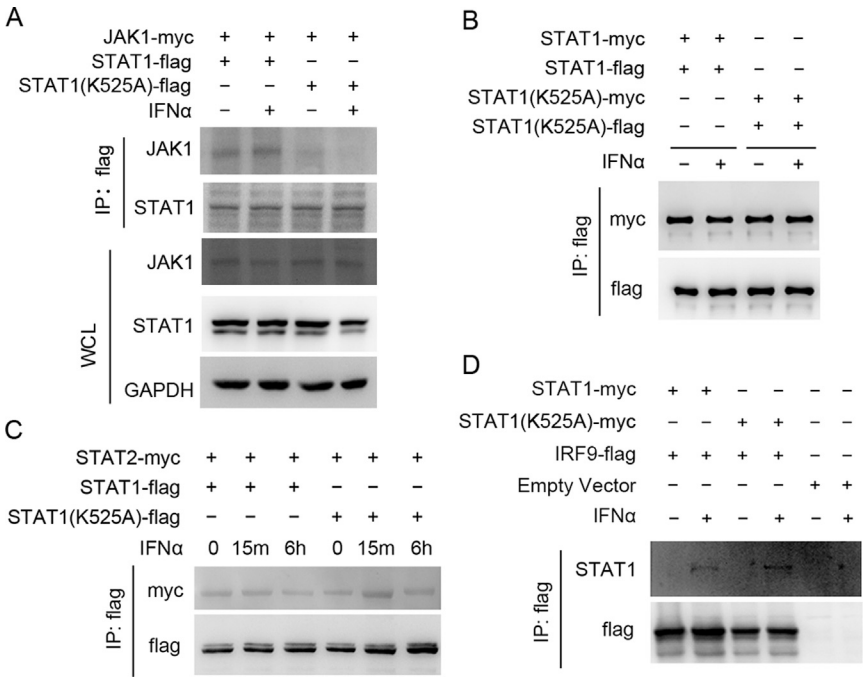

Figure S5. Methylation of Lysine 525 of STAT1 Is Necessary for Its Phosphorylation and Activation, Related to Figure 5

(A) IB analysis of JAK1 and STAT1 in the immunoprecipitates and the whole cell lysates of primary macrophages derived from $CD14^+$ human peripheral blood monocytes and co-transfected with myc-tagged JAK1 and flag-tagged STAT1-WT or STAT1-K525A, followed by IFNα treatment for 30 min.

(B) IB analysis of myc and flag in the immunoprecipitates of STAT1-KO cells co-transfected with both flag-tagged STAT1-WT and myc-tagged STAT1-WT or both flag-tagged STAT1-K525A and myc-tagged STAT1-K525A, followed by IFNα treatment for 30 min.

(C) IB analysis of myc and flag in the immunoprecipitates of STAT1-KO cells co-transfected with myc-tagged STAT2 and flag-tagged STAT1-WT or flag-tagged STAT1-K525A and stimulated with IFNα for the indicated time.

(D) IB analysis of STAT1 and flag in the immunoprecipitates of STAT1-KO cells co-transfected with flag-tagged IRF9 and myc-tagged STAT1-WT or myc-tagged STAT1-K525A, stimulated as in (A).

Similar results were obtained from three independent experiments with similar results.

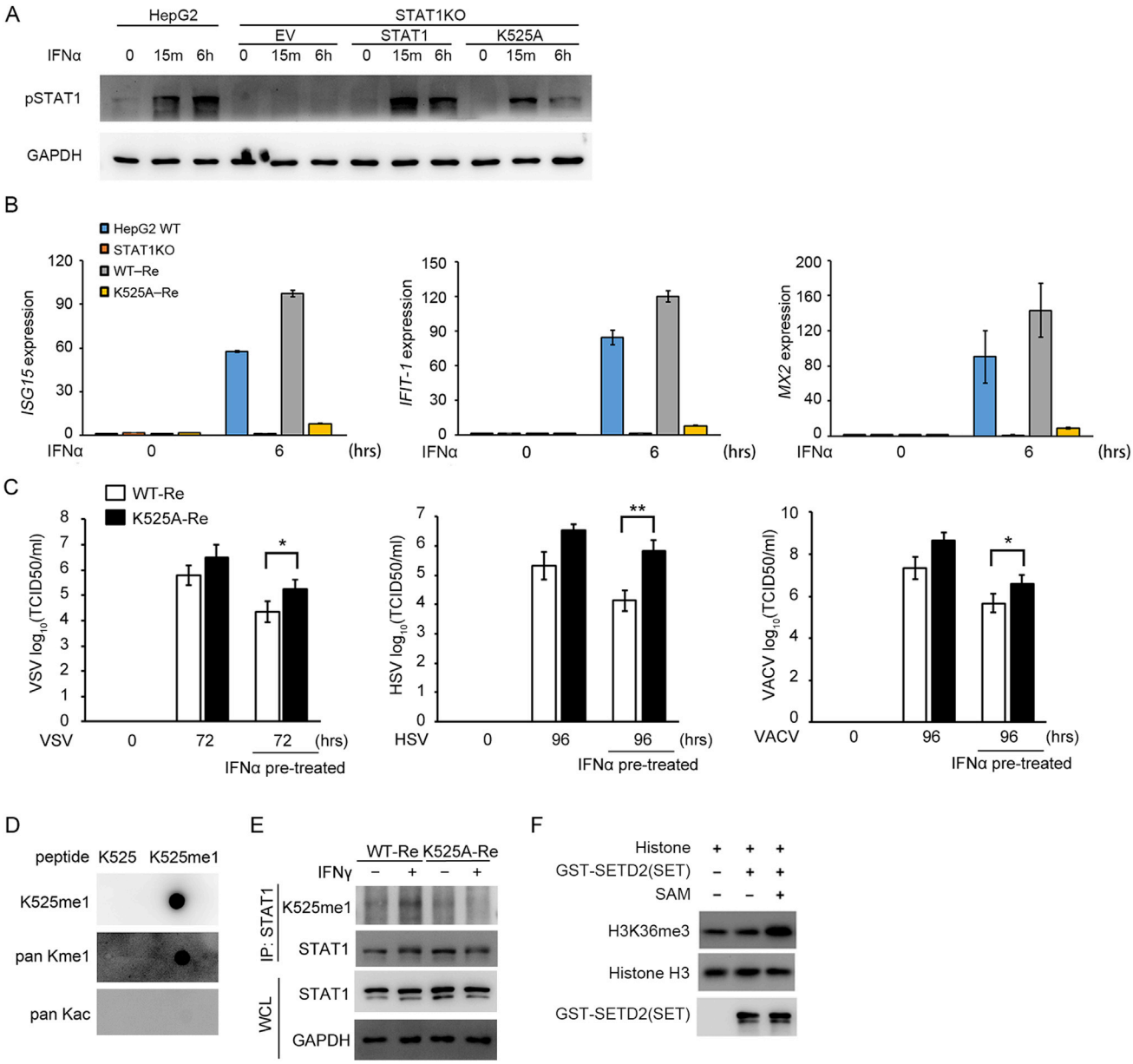

Figure S6. SETD2 Initiates K525me1 of STAT1 in Response to IFNα, Related to Figure 6

(A) IB analysis of pSTAT1 in whole-cell lysates of STAT1-KO cells rescued by stable expression of STAT1-WT or STAT1-K525A, treated with IFNα for the indicated time.

(B) qRT-PCR analysis of *ISG15*, *IFIT-1* and *MX2* expression in the rescued STAT1-KO cells treated with IFNα for 6 hr.

(C) $TCID_{50}$ assay of VSV, HSV and VACV titer in supernatants of WT-Re or K525A-Re cells with or without IFNα pretreatment and followed by VSV, HSV and VACV infection for 24 hr.

(D) Dot blot analysis of K525me1, pan-K-methyl and pan-Kac for the peptide containing methylated K525.

(E) IB analysis of K525me1 and STAT1 in the immunoprecipitates of the WT-Re or K525A-Re cells treated with IFNγ.

(F) In vitro methylation assay of purified histones. Histones purified from HepG2 cells were in vitro methylated with truncated SETD2 construct (1469-1724 aa.) using S-Adenosyl-L-Methionine (SAM). IB analysis of H3K36me3 antibody.

Data are representative of three independent experiments with similar results or shown as mean ± s.d. of three independent experiments (B, C). *$p < 0.05$, **$p < 0.01$.

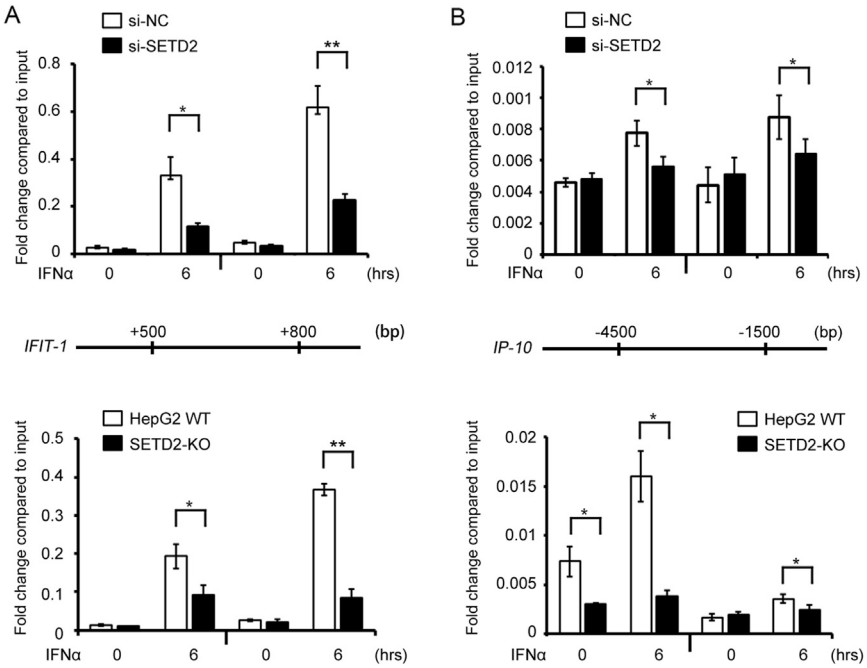

Figure S7. SETD2 Selectively Catalyzes H3K36me3 Modification of a Set of ISGs Gene Loci, Related to Figure 7

(A and B) ChIP analysis of H3K36me3 on gene loci of *IFIT-1* and *IP-10* in HepG2 cells transfected with (top) si-NC and si-SETD2 or (bottom) HepG2 WT and HepG2 SETD2-KO cells followed by 1,000 U/ml IFNα treatment for 6 hr. Locations of primers used for ChIP analysis in *IFIT-1* and *IP-10* genes (middle). Data are shown as mean ± s.d. of three independent experiments. $^{*}p < 0.05$, $^{**}p < 0.01$.